

Stony Brook University



OFFICIAL COPY

The official electronic file of this thesis or dissertation is maintained by the University Libraries on behalf of The Graduate School at Stony Brook University.

© All Rights Reserved by Author.

The Ahlfors Iteration for Conformal Mapping

A Dissertation Presented

by

Christopher Michael Green

to

The Graduate School

in Partial Fulfillment of the

Requirements

for the Degree of

Doctor of Philosophy

in

Mathematics

Stony Brook University

December 2011

Stony Brook University

The Graduate School

Christopher Michael Green

We, the dissertation committee for the above candidate for the Doctor of Philosophy degree, hereby recommend acceptance of this dissertation.

Christopher J. Bishop
Professor, Department of Mathematics
Dissertation Advisor

John Milnor
Distinguished Professor, Department of Mathematics
Chairman of the Defense

James Simons
Research Professor, Department of Mathematics

Andrew Mullhaupt
Research Professor, Applied Mathematics and Statistics
Stony Brook University

This dissertation is accepted by the Graduate School.

Lawrence Martin
Dean of the Graduate School

Abstract of the Dissertation

The Ahlfors Iteration for Conformal Mapping

by

Christopher Michael Green

Doctor of Philosophy

in

Mathematics

Stony Brook University

2011

The Riemann Mapping Theorem states that for any proper, simply connected planar domain there exists a conformal mapping from the disk onto the domain. But can this map be explicitly described? For general domains, there is no obvious answer. However, if the domain is the interior of a simple polygon, a convenient formula for the Riemann map was discovered independently by Schwarz and Christoffel. In this dissertation, we present a local quadratically convergent algorithm, the Ahlfors Iteration, based on the theory of quasiconformal maps in the plane, to compute the Schwarz-Christoffel mapping. This algorithm will also apply to a larger collection of simply connected Riemann surfaces. The Ahlfors Iteration improves upon current algorithms that compute the Schwarz-Christoffel map, in that, it is proven to converge, has a simple iterative form, and is easy to implement.

To my parents

Contents

List of Figures	vii
Acknowledgements	ix
Chapter 1. Introduction	1
1.1. Conformal Mappings and the Riemann Mapping Theorem	1
1.2. The Schwarz-Christoffel Formula	3
1.3. Other Methods	6
Chapter 2. Background	11
2.1. Polygonal Riemann Surfaces	11
2.2. Quasiconformal Mappings	14
2.3. Approximations and Triangulations	19
2.4. Quadrilaterals and Cross-Ratios	22
Chapter 3. The Ahlfors Iteration	25
3.1. Description of the Algorithm	25
3.2. Controlling Side Lengths	27
3.3. Triangles	38
Chapter 4. Implementing the Iteration	43
4.1. Delaunay Triangulations	43
4.2. Evaluating SC Mappings	44
4.3. Computing the Integral	49
4.4. Numerical Results	53
Bibliography	57

Appendix	60
A.1. Useful Formulas	60
A.2. Riemann Surfaces	61
A.3. Harmonic Measure	61

List of Figures

1.1 The conformal map z^2 .	1
1.2 A Schwarz-Christoffel map to a square.	4
1.3 A Schwarz-Christoffel map to a 12-gon.	5
1.4 Polygon with crowded parameters for large L .	5
1.5 Another polygon that has crowded parameters.	6
1.6 Avoiding the effects of crowding by using cross-ratios.	8
2.1 Two Riemann surfaces constructed from overlapping triangles.	11
2.2 A surface, P , with its embedded graph.	12
2.3 The same surface with two triangulations.	20
2.4 Q does not have a valid compatible triangulation.	21
2.5 A triangulated $P \in \mathcal{P}_{12}$ with Q_4 shaded.	22
3.1 The set Q_1 in gray.	29
3.2 $D(z)$ must lie in the shaded region if $z \in \cap Q_j$.	29
3.3 The neighboring sides of T are highlighted.	30
3.4 Bounding the parameter separation. The squares in $\partial\mathbb{D}$ are the third roots of unity.	31
3.5 Preserving the orientation of the triangle.	37
3.6 Triangles and angles in Lemma 3.3.1.	39
3.7 Triangles T and T' .	40
4.1 Flipping the diagonal.	44
4.2 Defining S^{-1} near corners.	47

4.3 Decomposing triangles for integration.	51
4.4 Above are the approximating polygons for each step of the Ahlfors Iteration and the target polygon. Below is the accuracy of the methods at each iteration.	54
4.5 The quadratic convergence of the Ahlfors Iteration is very pronounced for the polygon above.	55
4.6 Again, the Ahlfors Iteration converges in fewer steps.	56

Acknowledgements

The acknowledgements I would like to make must start with my advisor, Chris Bishop. Without his original interest in applying quasiconformal theory to the parameter problem, this dissertation would have never happened. His unwavering encouragement and readiness to answer and guide helped me through the dark thesis moments when solutions seemed non-existent.

I am grateful to the Stony Brook University Mathematics Department for the opportunity to continue my study of mathematics and the financial support to enable it.

Many thanks to the members of my dissertation committee, including John Milnor, James Simons, and Andrew Mullhaupt.

I would like to acknowledge the help of Raanan Schul and Jason Starr. Raanan's careful reading of this dissertation and insightful comments were invaluable. And Jason's guidance and advice at the beginning of my graduate career certainly set me on the right course.

Through the commiseration of my fellow graduate students over our shared experiences, I learned that I did not face the struggles and pitfalls of graduate school alone. And I thank them for that.

Finally, I must express my sincerest gratitude to my family. I thank my sisters, Jenna and Kassidy Green, for their support. I thank my grandmother, Johanna Green, for the innumerable lessons she has taught me through both her words and actions. And I thank my parents, Jane and Michael Green, for the stalwart example they have set for me and their trust in my decision to study mathematics, as opposed to other more "practical" pursuits.

CHAPTER 1

Introduction

1.1. Conformal Mappings and the Riemann Mapping Theorem

In this dissertation we seek to describe a certain class of *conformal mappings* defined on the complex plane, \mathbb{C} , or the Riemann sphere, $\hat{\mathbb{C}} = \mathbb{C} \cup \{\infty\}$. A C^1 mapping $f : U \rightarrow V$ of domains in \mathbb{C} is called *conformal* if for all $z = x + iy \in U$,

$$\frac{\partial}{\partial z} f(z) = f_z := \frac{1}{2} (f_x(z) - if_y(z)) \neq 0,$$

and

$$\frac{\partial}{\partial \bar{z}} f(z) = f_{\bar{z}} := \frac{1}{2} (f_x(z) + if_y(z)) = 0.$$

We say f is conformal in a neighborhood of ∞ if $f(1/z)$ is conformal in a neighborhood of 0. Thus, f is a holomorphic function whose complex derivative is everywhere nonzero. As a consequence, conformal mappings are homeomorphisms onto their images. An alternative and more geometric definition of conformality states that a C^1 function, f , is conformal at z if for every pair of oriented curves intersecting at z , the oriented angle is preserved under the image of f . Then f is said to be conformal in the whole domain if it preserves angles at every point. For a simple example of a conformal map, see Figure 1.1.

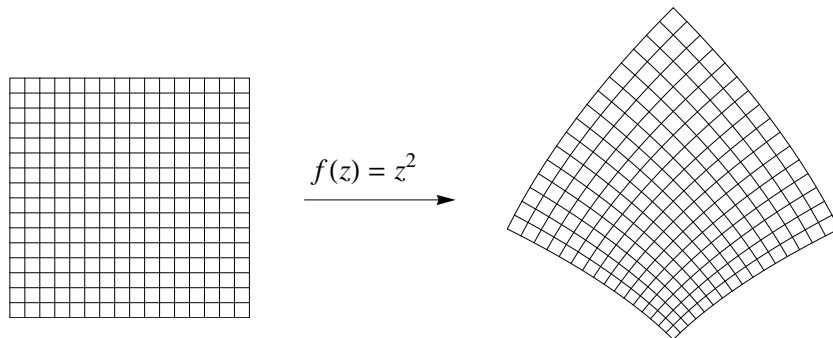


FIGURE 1.1. The conformal map z^2 .

Möbius transformations are a class of conformal maps defined on all of $\hat{\mathbb{C}}$. Fixing $a, b, c, d \in \mathbb{C}$ such that $ad - bc \neq 0$, the Möbius transformation

$$z \mapsto \frac{az + b}{cz + d}$$

is conformal. One can easily show that any Möbius transformation is a composition of a translation, a rotation, and a scaling, and that the image of circles and lines must also be circles or lines. Furthermore, the inverse of a Möbius transformation is still Möbius and so is the composition of two such maps.

An important Möbius transformation is the *Cayley transform* defined by

$$(1.1) \quad \mathcal{C}(z) = \frac{z - i}{z + i}.$$

When \mathcal{C} is restricted to $\mathbb{H} = \{z \in \mathbb{C} : \text{Im}z > 0\}$, it sends \mathbb{H} conformally onto \mathbb{D} . We say that two domains, U and V , are *conformally equivalent* if there exists a conformal mapping from U onto V . Therefore, \mathcal{C} gives us the conformal equivalence of \mathbb{H} and \mathbb{D} .

The preservation of angles definition of conformality allows the concept of conformal maps to be extended to higher dimensional Euclidean space, \mathbb{R}^n with $n \geq 3$. We can also extend Möbius transformations by defining them to be the composition of translations, scalings, orthogonal transformations, and inversions. In 1850, Liouville characterized conformal maps in \mathbb{R}^n , for $n \geq 3$, by proving that any conformal map defined on a domain in \mathbb{R}^n must be a Möbius transformation [25]. As a result, the unit ball in \mathbb{R}^n is conformally equivalent only to other balls and half-spaces. However, the equivalence issue is quite different in \mathbb{C} .

Riemann considered conformal equivalence of domains in \mathbb{C} in his 1851 thesis and gave a flawed proof that any simply connected domains other than \mathbb{C} and $\hat{\mathbb{C}}$ are conformally equivalent [19]. However, the statement is still true. It was not until Osgood's 1900 paper, [29], that a rigorous proof was given of what is now called the Riemann Mapping Theorem. The modern formulation states that for any simply connected domain, U , in $\hat{\mathbb{C}}$, whose boundary has at least two points, there exists a surjective conformal mapping $f : \mathbb{D} \rightarrow U$. Furthermore,

f is unique up to specifying that $f(0) = w_0 \in U$ and $f_z(0) > 0$. This is quite a remarkable result considering the infinite complexities one could construct for the boundary of U .

The downside of Riemann's theorem is that it proves the existence of such mappings but doesn't give any closed form solutions. However, from the work of Christoffel and Schwarz we have a convenient formula if our simply connected domain is the interior of a polygon.

1.2. The Schwarz-Christoffel Formula

Edwin Christoffel (1867) and Herman Amandus Schwarz (1869) independently discovered the explicit conformal map from the disk or the upper half plane to any simple polygon in the plane [13]. Any such mapping will be called a *Schwarz-Christoffel* (SC) map or formula. Let P denote the interior of a simple polygon with n vertices taken in counterclockwise order. Let $\alpha_j\pi > 0$ be the interior angle at the j th vertex so that we must have

$$\sum_{j=1}^n \alpha_j = n - 2.$$

Then the conformal map from \mathbb{D} to P must be given by

$$(1.2) \quad S(z) = A \int_0^z \prod_{j=1}^n \left(1 - \frac{\zeta}{p_j}\right)^{\alpha_j - 1} d\zeta + B,$$

for some $p_j \in \partial\mathbb{D}$, $A \in \mathbb{C} \setminus \{0\}$, and $B \in \mathbb{C}$. The integral can be taken along any path from 0 to z because the integrand is holomorphic in \mathbb{D} . Using the Cayley transform (1.1), we get a similar Schwarz-Christoffel formula from \mathbb{H} to P given by

$$(1.3) \quad S(z) = A \int_0^z \prod_{j=1}^n (\zeta - x_j)^{\alpha_j - 1} d\zeta + B,$$

where $x_j \in \mathbb{R}$. The constants may, of course, be different than those in (1.2). For proofs that these formulas do in fact give the correct conformal maps see [32].

The p_j (or x_j) above are called the *prevertices* or the *Schwarz-Christoffel parameters* for the polygon P . By Carathéodory's Theorem [16], S has a continuous extension to the boundary and, in fact, is a homeomorphism of the boundary of the domain onto ∂P . If v_j

is the j th vertex, then $S(p_j) = v_j$. Also, note that if \mathbb{H} is the domain of S , then ∞ can also be a parameter and, in this case, the corresponding term in the product in (1.3) is left out.

Suppose two SC maps, S_1 and S_2 , have image polygons, P_1 and P_2 , that differ by a Euclidean similarity, i.e. there are complex numbers a and b such that $m(P_1) = P_2$, where $m(z) = az + b$. Then $S_2^{-1} \circ m \circ S_1$ is a mapping of \mathbb{H} onto itself and can be extended to a conformal mapping of $\hat{\mathbb{C}}$ by the Schwarz reflection principle. The resulting map must be a Möbius transformation. Therefore, the parameters of S_1 and S_2 differ by a Möbius transformation. Conversely, if S is a SC transformation onto P and m is Möbius and sends \mathbb{H} to itself. Then $S \circ m$ is a conformal mapping of \mathbb{H} onto P and must be equal to a SC mapping with different parameters.

As an example of a SC mapping, let P be a square, then up to solving for the correct scaling constants, the SC map from the \mathbb{D} to P is

$$S(z) = \int_0^z \sqrt{(1-\zeta)(1+\zeta)(1-\zeta/i)(1+\zeta/i)} d\zeta,$$

with parameters $1, i, -1$, and $-i$. The image of \mathbb{D} under this map is shown in Figure 1.2. A more complicated SC mapping is seen in Figure 1.3.

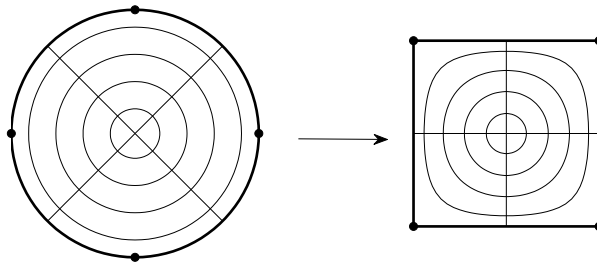


FIGURE 1.2. A Schwarz-Christoffel map to a square.

The Schwarz-Christoffel formula gives a compact and explicit expression for the Riemann map to a polygon *if* the parameters are known beforehand. However, this is almost never the case. Finding these parameters for a given polygon is known as solving the *parameter problem* and it is this problem that shall be considered in this dissertation. Note by the comments above, in order to find the parameters, it is enough to know them up to a Möbius transformation. Any Möbius transformation is uniquely determined by where it sends three

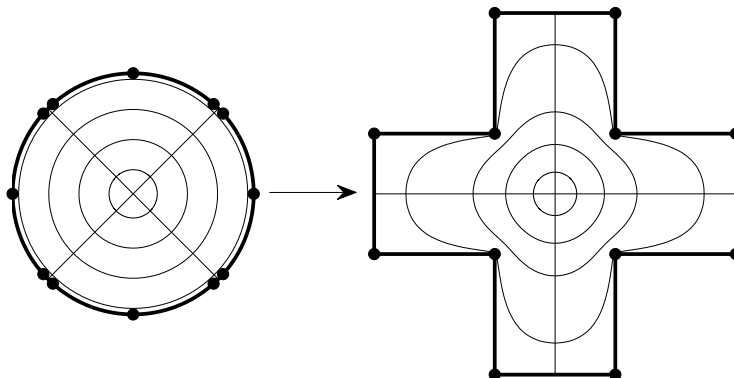


FIGURE 1.3. A Schwarz-Christoffel map to a 12-gon.

points, so fixing three points in the set of parameters uniquely determines the others. So instead of solving for the n parameters of an n -gon, we only need to find $n - 3$ parameters after fixing three.

Given a polygon and a fixed normalization of its parameters, one may wonder about the separation between parameters in $\partial\mathbb{D}$. It turns out that if the polygon is highly elongated, as in Figure 1.4, or has multiple “sections” connected by small pathways, as in Figure 1.5, the distance between parameters can become arbitrarily small, which poses an obvious difficulty if one wants to work with SC maps on a finite-precision computer. This bunching up of parameters is referred to as *crowding* in the literature.

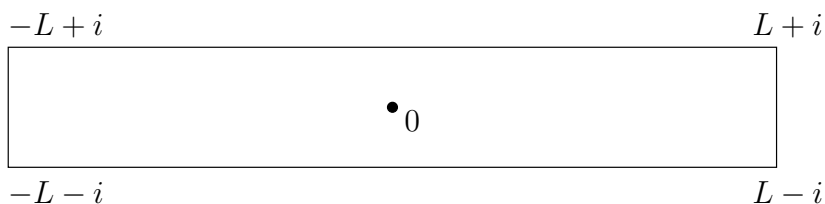


FIGURE 1.4. Polygon with crowded parameters for large L .

Parameter separation is intricately connected to the concept of harmonic measure (See Appendix A.3). Consider the polygon, P_L , in Figure 1.4 and suppose the SC mapping from the disk to P_L sends 0 to 0. Then the distance between consecutive parameters, measured in $\partial\mathbb{D}$ so that whole circle has length 1, is precisely the probability that a particle undergoing Brownian motion starting at 0 in P_L hits the side, E , of P_L corresponding to the chosen

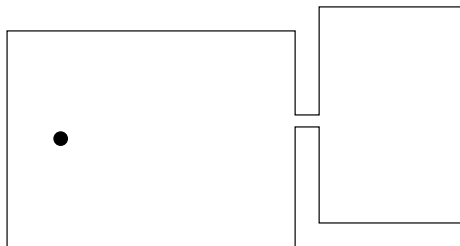


FIGURE 1.5. Another polygon that has crowded parameters.

consecutive parameters before hitting any other part of the boundary. This probability is also called the harmonic measure of E in P_L at 0. Furthermore, there are explicit estimates for the harmonic measure in this special case. Namely, let E be either of the vertical sides of P_L , then the harmonic measure at 0 of E and, hence, the parameter separation of the prevertices of E is $O(e^{-\frac{\pi}{2}L})$ [16]. In other words, the parameters converge together exponentially fast in L .

Similarly, for the polygon in Figure 1.5, if 0 was sent to the distinguished point in the left section of the polygon, then, qualitatively, the probability that a particle starting at 0 and undergoing Brownian motion would hit any of the sides in the right section of the polygon should be very small. And, hence, the parameters corresponding to the right section should be very close together on $\partial\mathbb{D}$. The new algorithm to be introduced below will attempt to avoid this crowding problem.

Other algorithms have been devised in the past to solve the parameter problem and a few will be reviewed in the next section. Each of the algorithms that follow suffer from one of two drawbacks; either the algorithm is easy to implement numerically but not proven to converge, or proven to converge but very difficult to implement. The new algorithm presented in this dissertation will be shown to converge and can be easily implemented on a computer.

1.3. Other Methods

Davis's Method [10] is a simple iterative scheme to find the SC parameters. Fix a polygon, P , with vertices v_1, \dots, v_n . Suppose $\theta_1^{(j)}, \dots, \theta_n^{(j)}$ are a guess for the arguments of

the SC parameters on $\partial\mathbb{D}$. Then using this guess and the angles from P , applying a SC map gives us another polygon with vertices $v_1^{(j)}, \dots, v_n^{(j)}$. We update the guess parameters by

$$\theta_{k+1}^{(j+1)} = \theta_k^{(j+1)} + k \left(\theta_{k+1}^{(j)} - \theta_k^{(j)} \right) \frac{|v_{k+1} - v_k|}{|v_{k+1}^{(j)} - v_k^{(j)}|},$$

where k is a normalization constant used in order to have the differences in consecutive angles sum to 2π . So, if a side of the guess polygon is too long (or too short) then the iteration compresses (or expands) the distance between the corresponding parameters. If one fixes a normalization of the parameters, then Davis' method can diverge, which was shown by Howell in [24]. However, it is not known if Davis's method converges if one allows a renormalization of the parameters.

The CRDT algorithm of Driscoll and Vavasis [14] is a very robust method for solving the parameter problem. It has not been proven to converge but there has yet be a case when it diverges, unlike Davis's method. CRDT stands for cross-ratios and Delaunay triangulations. Delaunay triangulations are a special kind of polygonal triangulation that maximizes the angles in the triangles (See Section 4.1). Cross-ratios are also important to the algorithm presented in this dissertation and are detailed in Section 2.4. In short, a cross-ratio is a unique complex number assigned to an ordered 4-tuple of distinct points in $\hat{\mathbb{C}}$.

The CRDT algorithm utilizes cross-ratios in the following way. Suppose we have a n -gon, P , with a fixed triangulation. Then from the $n-2$ triangles one can form $n-3$ quadrilaterals (See Section 2.4). Taking the cross-ratios of the prevertices of each quadrilateral gives $n-3$ real numbers. It is enough to know these numbers and the quadrilateral structure to recreate the polygon and prevertices. So, for a given polygon and quadrilateral decomposition solving the parameter problem is the same as solving for the appropriate cross-ratios. Let F denote the function from the parameter cross-ratios to the cross-ratio of the corresponding quadrilateral in the approximate polygon. If \mathbf{z}_0 is the set of cross-ratios of the quadrilaterals in P and \mathbf{c}_0 is the correct parameter cross-ratios, then \mathbf{c}_0 is a solution to the nonlinear equation $F(\mathbf{c}) - \mathbf{z}_0 = 0$. One can then use generic numerical nonlinear solvers to find the solution.

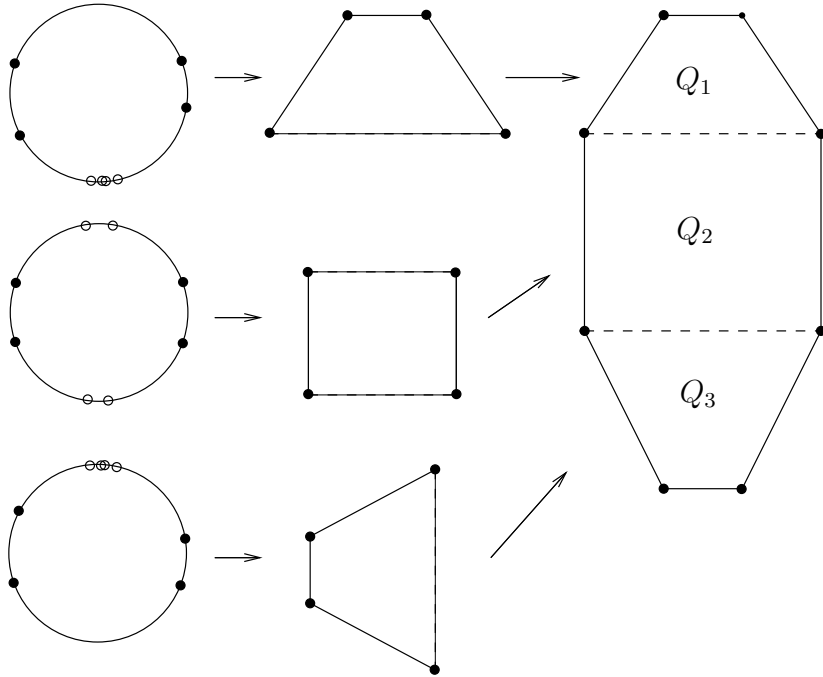


FIGURE 1.6. Avoiding the effects of crowding by using cross-ratios.

CRDT avoids the crowding problem described above by renormalizing the parameters in $\partial\mathbb{D}$ as follows. Suppose we have an n -gon, P , with quadrilaterals, Q_1, \dots, Q_{n-3} , and we know the corresponding cross-ratios of the prevertices of each Q_j . From these cross-ratios, we can construct P up to a similarity. To do so, for each Q_j , normalize three of its prevertices in $\partial\mathbb{D}$. Then from the cross-ratios, the fourth prevertex, as well as the rest of the parameters of P , are uniquely determined (See Section 2.4). Furthermore, one can compute an accurate image of the vertices of Q_j . Fixing Q_1 , we can then reassemble overlapping quadrilaterals using affine maps to construct an accurate image of P . See Figure 1.6. This may not have been possible if we had fixed one normalization of the prevertices of P because severe crowding could cause some parameters to be indistinguishable to a finite-precision computer.

Bishop's Fast Mapping Algorithm [6] (FMA) solves the parameter problem for an n -gon in $O(n)$ time in a much different way than CRDT and Davis's method. Both of the previous schemes take a parameter guess, apply a SC mapping to get another polygon, and use some geometric characteristic to compare it to the target polygon in order to update the guess. For CRDT, the characteristic is the cross-ratio of quadrilaterals, and for Davis's

method it's side length. Instead of taking a conformal map to a guess polygon, the FMA creates a quasiconformal map (See Section 2.2 for an overview of quasiconformal mappings in the plane) from \mathbb{H} to the target polygon sending the prevertex guess to the corresponding vertex in P . Let $f : \mathbb{H} \rightarrow P$ be the constructed map and $S : \mathbb{H} \rightarrow P$ is the correct SC mapping. Then $g = S^{-1} \circ f : \mathbb{H} \rightarrow \mathbb{H}$ is a quasiconformal mapping of \mathbb{H} that sends the guess prevertices to the true prevertices and satisfies a partial differential equation called the Beltrami equation (2.7). The FMA partially solves this equation to obtain an approximation \tilde{g} to g such that \tilde{g} maps the guess prevertices closer to the true ones in a quasiconformal sense. A new mapping f is then constructed and the algorithm iterates again.

The FMA has many advantages over the previous algorithms. For one, Bishop proves that it globally converges to the correct parameters, which makes it the only proven globally convergent algorithm for the parameter problem. Another advantage is that it is a linear time algorithm depending only on the number of vertices. However, the FMA is highly complex and has yet to be implemented.

The algorithm presented in this dissertation, the Ahlfors Iteration, will draw from the advantages of each of the three previously presented methods. Like Davis's method, it will have a simple iterative structure. It will incorporate cross-ratios of quadrilaterals as in CRDT, which will avoid reliance on a fixed embedding of prevertices and, thus, avoid crowding. Like the FMA, it will be quadratically convergent and rely heavily on the theory of quasiconformal mappings. However, the convergence will be local in the sense that it will depend on the particular target polygon.

We would be remiss not to mention some of the myriad applications of Schwarz-Christoffel mappings. The classical use of SC mappings is the solution of Laplace's equation in mathematical physics, solutions to which are invariant under conformal mappings [30], [13]. Other physical applications include electromagnetics, heat transfer, and fluid flow [30]. SC maps can also be used in meshing problems by first meshing the disk and then transforming the mesh using a SC map [7]. Schwarz-Christoffel mappings can even be used for shape analysis in computer vision [31]. Of course, in order to use a SC map one needs the parameters and

before detailing our new algorithm to find them we must review some background material.

CHAPTER 2

Background

2.1. Polygonal Riemann Surfaces

The classical Schwarz-Christoffel formula describes the conformal map from the disk or half-plane to the interior of any simple polygon in the plane. However, we do not need to restrict ourselves to planar domains but can apply the algorithm to come to a class of Riemann surfaces, whose construction we now discuss. For general background on Riemann surfaces see Appendix A.2. The surfaces we create will be assembled from triangles in \mathbb{C} . A triangle in the plane has two possible orientations based upon the ordering of its vertices. We will always use counterclockwise oriented triangles with respect to its interior.

Suppose two triangles, T_1 and T_2 , in \mathbb{C} share two vertices such that $T_1 \cap T_2$ is the common line segment between those vertices. We identify points along these corresponding edges to create a quadrilateral. Continuing in this way we “glue” other triangles to the *boundary* of the surface already constructed such that only one edge of a new triangle is identified with the previous surface. See Figure 2.1. The interior of the resulting space is a Riemann surface. See [3] for a slight generalization.

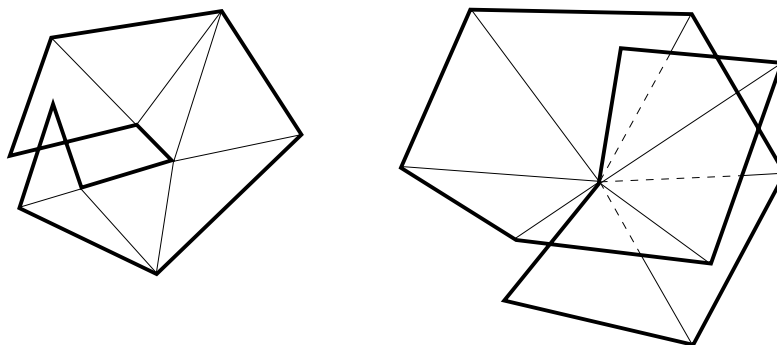


FIGURE 2.1. Two Riemann surfaces constructed from overlapping triangles.

A natural graph structure arises from these surfaces if each triangle represents a node and nodes are connected if triangles share an edge. In fact, we can embed such a graph in the surface by letting the centroid, the average of the vertices in \mathbb{C} , of each triangle be the node and connect centroids if edges intersect. See Figure 2.2. For a given surface, P , denote this graph by G_P .

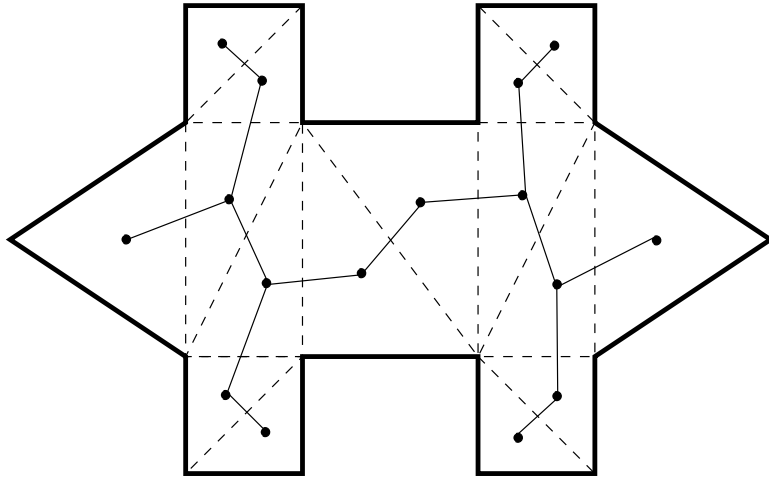


FIGURE 2.2. A surface, P , with its embedded graph.

We now define the set of surfaces we will use throughout this dissertation. For positive integers $n \geq 3$, let \mathcal{P}_n denote the set of all Riemann surfaces constructed as above with $n - 2$ triangles such that for all $P \in \mathcal{P}_n$, G_P is a tree. A surface in \mathcal{P}_n will be called a *polygonal Riemann surface*. Recall that by definition a graph is a tree if any two nodes can be connected by a unique non-self-intersecting path.

LEMMA 2.1.1. *If $P \in \mathcal{P}_n$, then P is simply connected.*

PROOF. This lemma follows from a quick induction argument. If $n = 3$, then $P \in \mathcal{P}_n$ is just a planar triangle so must be simply connected. If $n > 3$, then $P \in \mathcal{P}_n$ can be written as a union $T \cup S$ where T is a triangle and $S \in \mathcal{P}_{n-1}$ such that only one edge of T is identified with a side of the boundary of S . Assume for induction that S is simply connected. $T \cap S$ is a line segment and, hence, path connected. Since P is the union of simply connected sets whose intersection is path connected, P must also be simply connected by the van Kampen theorem [21]. \square

As a consequence of the lemma, the boundary of any polygonal Riemann surface must be a closed polygonal curve. The angle at any vertex is the sum of the angles of the triangles that share the vertex in the construction of the surface. Furthermore, note that every simple n -gon is also in \mathcal{P}_n because every polygon can be triangulated into $n - 2$ triangles.

Why is it necessary to know that every surface in \mathcal{P}_n is simply connected? Well, it follows from the Uniformization Theorem that every P in \mathcal{P}_n must be conformally equivalent to either the open unit disk, the complex plane, or the Riemann sphere. For a proof of the Uniformization Theorem see [15] and for its history see [19]. Since P is not compact it cannot be conformally equivalent to $\hat{\mathbb{C}}$. Furthermore, there can't exist a conformal mapping from P to \mathbb{C} . To see this note that P is constructed from finitely many planar triangles. Each of these triangles can be projected back onto \mathbb{C} such that its angles are preserved and overlapping edges are still overlapping in \mathbb{C} . Denote this projection by $\pi_P : P \rightarrow \mathbb{C}$. If there was a conformal mapping from \mathbb{C} to P , then composing with π_P would give a bounded holomorphic function on \mathbb{C} . By Liouville's theorem on bounded entire functions, such a function must be constant, which gives us a contradiction. We conclude that for every $P \in \mathcal{P}_n$ there must be a conformal mapping $S : \mathbb{D} \rightarrow P$.

For most simply connected domains we don't have an explicit equation for the conformal mapping guaranteed by the Uniformization Theorem. The classical Schwarz-Christoffel formula gives such an equation for $P \in \mathcal{P}_n$ if P is a planar polygon. Luckily, the Schwarz-Christoffel formula (1.3) extends to all $P \in \mathcal{P}_n$. For a general P , the interior angles are not restricted to be less than 2π but can be arbitrarily large. The generalization of the Schwarz-Christoffel formula to Riemann surfaces was proved independently by Gilbarg [17] and Goodman [18].

The goal of the Ahlfors Iteration is to find the correct Schwarz-Christoffel parameters for a given polygon $P \in \mathcal{P}_n$ up to a Möbius transformation. Therefore, normalizing the parameters to some convenient choices will not affect the outcome. We will often use \mathbb{D} as our domain for a map $S : \mathbb{D} \rightarrow P$ and normalize three of the parameters to the three third roots of unity, ξ_k .

If we make a guess of the true parameter values we most likely will not have the correct ones or be correct up to a Möbius transformation. But how can we measure how poor our guess is? We could use the Euclidean distance from a fixed normalization. But this requires that the target parameters are known beforehand, which is certainly not always true. There is a generalization of conformal mappings, called quasiconformal mappings, that will not only give us a practical way of measuring the error of a particular guess, but also, it is from the theory of such mappings that leads to the Ahlfors Iteration.

2.2. Quasiconformal Mappings

There are three common and equivalent ways to define a quasiconformal mapping of domains in \mathbb{C} . They are referred to as the *metric*, *analytic*, and *geometric* definitions. Suppose $f : \Omega \rightarrow \Omega'$ is a homeomorphism. The metric definition says that f is K -quasiconformal (or K -QC) for some $K \geq 1$ if for all $x \in \Omega$

$$(2.1) \quad \limsup_{r \rightarrow 0} \frac{\sup\{|f(x) - f(y)| : |x - y| \leq r\}}{\inf\{|f(x) - f(y)| : |x - y| \leq r\}} \leq K.$$

The metric definition intuitively states that quasiconformal mappings send small circles to small ellipses with bounded eccentricity, which is an obvious generalization of conformal mappings, which send small circles to small circles.

The map f is K -quasiconformal by the analytic definition if f is absolutely continuous on almost every horizontal and vertical lines with respect to Lebesgue measure of any rectangle contained in Ω and

$$(2.2) \quad |f_{\bar{z}}| \leq k |f_z|,$$

where $k = \frac{K-1}{K+1}$, holds almost everywhere.

For the geometric definition, we first define the *modulus* of a family of curves, Γ , in Ω by

$$(2.3) \quad \text{mod}(\Gamma) = \inf_{\rho} \frac{A(\rho)}{L(\rho)^2},$$

where ρ must be a non-negative Borel measurable real-valued function on Ω such that $A(\rho) = \int_{\Omega} \rho^2 dA$ is positive and finite, and $L(\rho) = \inf_{\gamma \in \Gamma} \int_{\gamma} \rho ds$. Then f is K -quasiconformal if for every family of curves Γ in Ω , we have

$$(2.4) \quad K^{-1} \text{mod}(f(\Gamma)) \leq \text{mod}(\Gamma) \leq K \text{mod}(f(\Gamma)).$$

The geometric definition is certainly not as intuitive as the metric definition, but from it, simple properties of quasiconformal mappings are easily deduced [1]. First, composition with conformal mappings preserves K -quasiconformality. Second, the composition of a K_1 -QC mapping and a K_2 -QC mapping gives a $K_1 K_2$ -QC mapping. Finally, if f is K -quasiconformal, then f^{-1} is as well. Also, being a 1-QC map is equivalent to conformality, justifying the claim that quasiconformality generalizes conformality.

Since the algorithm will apply not only to planar polygons, but also to polygonal Riemann surfaces, we need to define quasiconformal mappings of Riemann surfaces. A homeomorphism f between two Riemann surfaces, P_1 and P_2 , is called K -quasiconformal if for charts h_1 and h_2 on P_1 and P_2 , respectively, the mapping $h_2 \circ f \circ h_1^{-1}$ is K -quasiconformal in the domain in \mathbb{C} where it is defined. Thus, if the surfaces are planar, then h_1 and h_2 are the identity and we are left with the planar definition of quasiconformality.

Given a K -QC mapping, f , define its *complex dilatation*, μ_f , by

$$(2.5) \quad \mu_f = \frac{f_{\bar{z}}}{f_z}.$$

The analytic definition tells us that μ_f satisfies

$$(2.6) \quad \|\mu_f\|_{\infty} \leq \frac{K-1}{K+1},$$

where $\|\cdot\|_{\infty}$ is the usual essential supremum norm. Conversely, if we are given a measurable function, μ , on \mathbb{C} such that $\|\mu\|_{\infty} \leq k < 1$, then there exists a quasiconformal mapping, f , satisfying the *Beltrami equation*

$$(2.7) \quad f_{\bar{z}} = \mu f_z.$$

The existence of such an f is called the *Measurable Riemann Mapping Theorem* and was first proved by Morrey in [28]. The solution to (2.7) is unique if we require it to fix three points (See Section V in [1]).

Let's take a look at a simple yet fundamental example of a quasiconformal map.

EXAMPLE 2.2.1. Given two triangles, T and T' , we can always find a conformal mapping from one to the other which sends the vertices to the vertices by composing a SC map with the inverse of another. If we allow the mapping to be quasiconformal instead, then a simple formula results. In particular, it takes the form of an affine complex mapping

$$(2.8) \quad L(z) = az + b\bar{z} + c,$$

where $a, b, c \in \mathbb{C}$. To see that such a function is QC assume by composing with linear Möbius transformations that the vertices of T are $0, 1$, and w , and they are mapped by L to $0, 1$, and w' , respectively. We assume the vertices are listed in a counterclockwise order so that w and w' lie in \mathbb{H} . Then $c = 0$, $a + b = 1$, and $w' = aw + b\bar{w}$. Solving for a and b yields $a = (w' - \bar{w})/(w - \bar{w})$ and $b = (w - w')/(w - \bar{w})$. Then the dilatation of L satisfies

$$(2.9) \quad |\mu_L| = \left| \frac{b}{a} \right| = \frac{|w - w'|}{|w' - \bar{w}|} < 1$$

since $w, w' \in \mathbb{H}$. We conclude that affine mappings between triangles are in fact quasiconformal.

It also follows that affine complex mappings send quadrilaterals to quadrilaterals. In fact, if we have two rectangles R and R' with lower left corners at the origin with side lengths a, b and a', b' , respectively, and assume that $a/b \leq a'/b'$, then the quasiconformal mapping from R to R' is given by

$$f(z) = \frac{1}{2} \left(\frac{a'}{a} + \frac{b'}{b} \right) z + \frac{1}{2} \left(\frac{a'}{a} - \frac{b'}{b} \right) \bar{z}.$$

It is easy to show that f is a $(a'/b')/(a/b)$ -QC mapping. See [1] for a more detailed discussion.

It is often useful to extend QC mappings of \mathbb{H} onto itself to the lower half plane by a reflection. Let $f : \mathbb{H} \rightarrow \mathbb{H}$ be QC and define for $z \in \mathbb{H}^-$, $f(z) = \overline{f(\bar{z})}$. Then the resulting

mapping has dilatation, μ_f , in \mathbb{H} and in \mathbb{H}^- , it is given by $\overline{\mu_f(\bar{z})}$. The map f must also be continuous up to the real line, which follows easily from Mori's Theorem on the Hölder continuity of QC mappings [1].

Suppose f is a quasiconformal mapping of the plane fixing 0, 1, and ∞ . In [1], Ahlfors derives the following expansion of f on \mathbb{D} from the generalized Cauchy integral formula. If $|w| < 1$ then

$$(2.10) \quad f(w) = w - \frac{1}{\pi} \iint_{|z|<1} f_{\bar{z}}(z) R(z, w) dx dy - \frac{1}{\pi} \iint_{|z|<1} \frac{\check{f}_{\bar{z}}(z)}{\check{f}(z)^2} z S(z, w),$$

where

$$(2.11) \quad R(z, w) = \frac{1}{z-w} - \frac{w}{z-1} + \frac{w-1}{z} = \frac{w(w-1)}{z(z-1)(z-w)},$$

$S(z, w) = \frac{w^2}{1-zw} - \frac{w}{1-z}$, and $\check{f}(z) = 1/f(\frac{1}{z})$. From (2.10) Bishop arrives at the following result.

LEMMA 2.2.2 (Bishop [4]). *Fix $\rho \geq 1$. There is a $0 < k_1 < 1$ and a $C_1 = C_1(\rho) < \infty$ so that the following holds. Suppose that f is a quasiconformal mapping of the plane to itself fixing 0, 1, and ∞ , and the Beltrami coefficient of f is μ with $\|\mu\|_\infty \leq k_1$. Then*

$$(2.12) \quad \left| f(w) - \left[w - \frac{1}{\pi} \int_{\mathbb{C}} \mu(z) R(z, w) dx dy \right] \right| \leq C_1 \|\mu\|_\infty^2,$$

for all $|w| \leq \rho$, where R is as in (2.11).

Inequality 2.12 plays a central role in the Ahlfors Iteration described below because the term in brackets gives a first approximation to the actual QC map f . So, if we can compute the integral we'll have an approximation to the map. However, this lemma leaves something to be desired because it says that the bracketed term and f are close in the Euclidean metric but this tells us little if we don't already know the values of $f(w)$. One deduces from Lemma 2.2.2 that if our quasiconformal constant is small enough, then there exists a $C_2 > 0$ such that for every $|w| \leq \rho$,

$$(2.13) \quad |f(w) - w| \leq C_2 \|\mu_f\|_\infty.$$

It will also be necessary to know how a quasiconformal mapping of the disk to itself behaves on the boundary if it fixes the third roots of unity.

LEMMA 2.2.3. *There exists a $0 < k_2 < 1$ and $C_3 < \infty$ such that if $f : \mathbb{D} \rightarrow \mathbb{D}$ is a $(1 + \epsilon)$ -quasiconformal mapping fixing the third roots of unity with $\epsilon \leq k_2$, then for all $\zeta \in \partial\mathbb{D}$*

$$(2.14) \quad |f(\zeta) - \zeta| \leq C_3\epsilon.$$

PROOF. The proof is easier if we assume f fixes $-1, -i$, and 1 instead. We can make this assumption since we can always apply Möbius transformations of the disk to itself, which can distort points on the boundary by a bounded amount.

Let $k_2 = k_1$ from Lemma 2.2.2 and assume f is a $(1 + \epsilon)$ -QC mapping with $\epsilon \leq k_2$. Further, let $C_3 = 2C_2$ from (2.13). Recall from (1.1) that the Cayley transform, \mathcal{C} , sends \mathbb{H} to \mathbb{D} and $0, 1, \infty$ to $-1, -i, 1$, respectively. We may write $f = \mathcal{C} \circ F \circ \mathcal{C}^{-1}$, where $F : \mathbb{H} \rightarrow \mathbb{H}$ fixes $0, 1$, and ∞ , and is also $(1 + \epsilon)$ -q.c. Given $\zeta \in \partial\mathbb{D}$, we write $\zeta = \mathcal{C}(x)$ for x real. Then

$$\begin{aligned} |f(\zeta) - \zeta| &= |\mathcal{C}(F(x)) - \mathcal{C}(x)| \\ &= \frac{2|F(x) - x|}{|F(x) + i||x + i|}. \end{aligned}$$

If $|x| \leq 1$, then the denominator above is at least 1 since x and $F(x)$ are both real, and we can apply (2.13) to the numerator to get our result.

Assume $|x| > 1$ and consider $\check{F}(z) = 1/F(1/z)$. Then \check{F} is $(1 + \epsilon)$ -QC from \mathbb{H} to \mathbb{H} and fixes $0, 1$, and ∞ . So

$$\begin{aligned} |\check{F}(1/x) - 1/x| &= |1/F(x) - 1/x| \\ &= \frac{|F(x) - x|}{|F(x)||x|} \\ &\leq C_2\epsilon, \end{aligned}$$

where the inequality follows from (2.13). We conclude

$$\begin{aligned} |f(\zeta) - \zeta| &= \frac{2|F(x) - x|}{|F(x) + i||x + i|} \\ &\leq 2\frac{|F(x) - x|}{|F(x)||x|} \\ &\leq C_3\epsilon. \end{aligned}$$

□

Quasiconformal mappings come up in many areas of mathematics including geometric function theory, dynamics, and low-dimensional topology (See the supplemental chapters in [1] and the references presented there or [23]). The definition of quasiconformality can even be extended to arbitrary metric spaces [22]. For the origins of the theory of 2 dimensional quasiconformal mappings see [1] or [27] and for higher dimensions see [35]. For a modern treatment of planar QC mappings see [2].

2.3. Approximations and Triangulations

We claimed earlier that quasiconformal maps could provide a way to measure the error between a guess of the SC parameters and the true parameters for a polygonal Riemann surface. In order to accomplish this we must define a metric on \mathcal{P}_n . Suppose $P, Q \in \mathcal{P}_n$ and define

$$(2.15) \quad d_{QC}(P, Q) = \inf\{\log K : \exists K\text{-QC} \\ f : P \rightarrow Q \text{ sending vertices to vertices}\}.$$

It follows that d_{QC} is a metric on \mathcal{P}_n if we identify surfaces up to conformal transformations. It is clear that d_{QC} is non-negative. If $d_{QC}(P, Q) = 0$, then there is a 1-QC map between them, otherwise known as a conformal map between our two surfaces. But we identified conformally equivalent surfaces, so $P = Q$. Since inverse mappings are also quasiconformal with the same constant, d_{QC} is reflexive. Using the fact that composing QC maps results in multiplying their QC constants gives the triangle inequality.

Let $P \in \mathcal{P}_n$ and $\epsilon > 0$, we say that $\tilde{P} \in \mathcal{P}_n$ is an ϵ -*approximation* of P if there exists a $(1 + 2\epsilon)$ -quasiconformal mapping from \tilde{P} to P sending the vertices of \tilde{P} to the vertices of P and the interior angles at corresponding vertices are equal. Using our metric defined in (2.15), an ϵ approximation satisfies $d_{QC}(P, \tilde{P}) \leq \log(1 + 2\epsilon)$. If f is $(1 + 2\epsilon)$ -QC, then using inequality (2.6) we have $\|\mu_f\|_\infty \leq \epsilon$.

If $P \in \mathcal{P}_n$ and we have a guess for the SC parameters, then applying a SC mapping using the guess and the corresponding angles of P gives some other $\tilde{P} \in \mathcal{P}_n$. If we can construct a QC mapping, $f : \tilde{P} \rightarrow P$, then we will have an upper bound on $d_{QC}(P, \tilde{P})$. If the QC constant is not too big, then Lemma 2.2.3 gives a uniform approximation on how close the guess SC parameters are to the true parameters for P .

To construct a QC map between polygonal Riemann surfaces we will first need to decompose the surfaces into triangles. This is easy since we first constructed the surfaces from triangles. A *triangulation*, \mathcal{T} , of $P \in \mathcal{P}_n$ is a set of $n - 2$ triangles in \mathbb{C} from which the surface P can be reconstructed. A triangulation does not have to be unique because the same surface can be constructed from different triangles, as we can see in Figure 2.3.

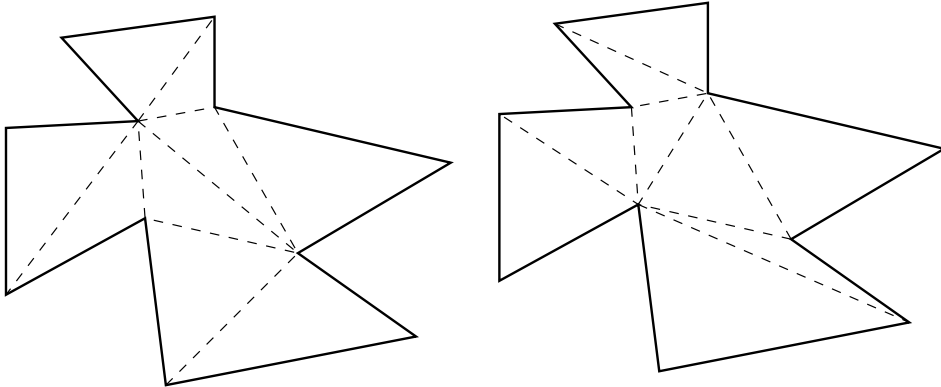


FIGURE 2.3. The same surface with two triangulations.

Example 2.2.1 shows how easy it is to write down (and compute) a quasiconformal map between triangles. We want to do the same thing with polygonal Riemann surfaces. Given $P, Q \in \mathcal{P}_n$ with vertices $\{v_j\}$ and $\{w_j\}$, respectively, and a triangulation \mathcal{T} of P , a triangulation \mathcal{T}' of Q will be called *compatible* with \mathcal{T} if for each triangle $T_j \in \mathcal{T}$ with vertices $v_{j_1}, v_{j_2}, v_{j_3}$, the triangle with vertices $w_{j_1}, w_{j_2}, w_{j_3}$ is in \mathcal{T}' . It is certainly not true

that Q must have a compatible triangulation with \mathcal{T} even if they have the same interior angles as Figure 2.4 shows.

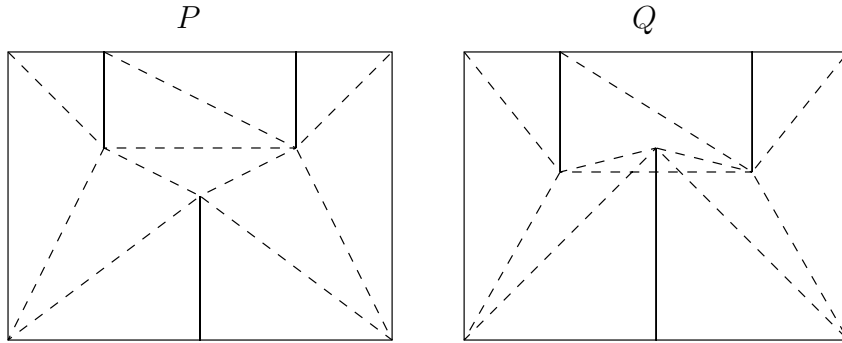


FIGURE 2.4. Q does not have a valid compatible triangulation.

If P and Q have a compatible triangulation, then we may define a piecewise affine map, $L : P \rightarrow Q$, sending the triangles of P to the compatible triangles in Q . It is easy to check that individual maps must agree on overlapping edges. Then L is quasiconformal and

$$d_{QC}(P, Q) \leq \log \left(\frac{1 + \|\mu_L\|_\infty}{1 - \|\mu_L\|_\infty} \right).$$

So, if we have a guess for the SC parameters and the resulting surface has a compatible triangulation with some fixed triangulation of the target surface, we can use the mapping L to get an explicit estimate for how far away our guess is to being a conformal image of the target.

The importance of a compatible triangulation of an ϵ -approximation should be apparent and a simple condition is needed to guarantee compatibility. Let $P \in \mathcal{P}_n$ and consider its image in \mathbb{C} under the projection map, π_P . Since π_P sends the triangles in P to their original images in \mathbb{C} , one could rebuild P from $\pi_P(P)$. But if a vertex of a triangle in $\pi_P(P)$ is perturbed, can we still construct a polygonal Riemann surface from the collection of triangles? If so, then the resulting surface has a compatible triangulation with P . Now, all that was required in the construction of our surfaces was that adjacent triangles be non-overlapping when we “glue” them in \mathbb{C} . Therefore, if a vertex is perturbed the only way we could go wrong is if one of the triangles changes orientation as was the case in Figure 2.4.

We've proved the following lemma.

LEMMA 2.3.1. *Let $P_1, P_2 \in \mathcal{P}_n$ and fix a triangulation \mathcal{T} of P_1 . Suppose that for every triangle in \mathcal{T} with counterclockwise vertices v_1, v_2 , and v_3 , and corresponding vertices w_1, w_2 , and w_3 in P_2 , the triples $\{\pi_{P_1}(v_j)\}$ and $\{\pi_{P_2}(w_j)\}$ have the same orientation. Then there exists a compatible triangulation of P_2 with \mathcal{T} .*

2.4. Quadrilaterals and Cross-Ratios

Let $P \in \mathcal{P}_n$ and fix a triangulation \mathcal{T} . Consider the $n-3$ diagonals, d_j , in P corresponding to the sides in the interior of P of the triangles in \mathcal{T} . Let Q_j be the quadrilateral formed by taking the union of the two triangles in \mathcal{T} that share the diagonal d_j . We see the set up in Figure 2.4.

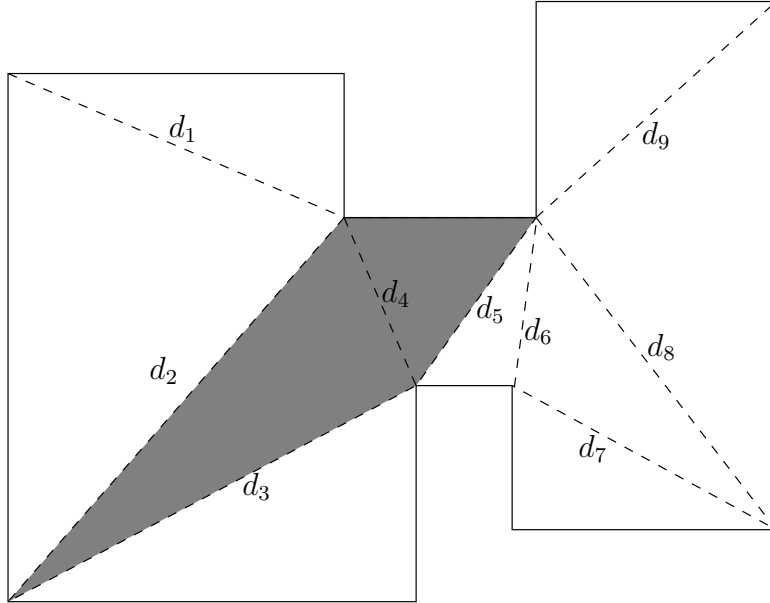


FIGURE 2.5. A triangulated $P \in \mathcal{P}_{12}$ with Q_4 shaded.

Each quadrilateral will be assumed to be positively (counterclockwise) oriented. It is easy to see that if $v_{j_1}, v_{j_2}, v_{j_3}$, and v_{j_4} are the vertices of Q_j in counterclockwise order such that v_{j_1} and v_{j_3} are the endpoints of d_j then, v_{j_2} and v_{j_4} lie on separate components of $\partial P \setminus \{v_{j_1} \cup v_{j_3}\}$. From this we deduce, that if the prevertices of v_{j_1}, v_{j_3} , and v_{j_4} are normalized to 0, 1, and ∞ , respectively, then we must have $v_{j_2} \in (0, 1)$, a fact that will be used often in the algorithm to

come. We take the time to note that if we fix $P \in \mathcal{P}_n$ and let \mathcal{Q} denote its set of quadrilaterals with respect to a fixed triangulation, then if $\tilde{P} \in \mathcal{P}_n$ has a compatible triangulation, \tilde{P} can be given the same quadrilateral structure.

Another concept needed is that of the cross-ratio of four points. If $P \in \mathcal{P}_n$ and $S : \mathbb{H} \rightarrow P$, then, as seen earlier, we can describe S fully if we know the prevertices of P up to a Möbius transformation. There is another equivalent means by which to encode the prevertex data and, hence, the Riemann map. We follow closely the method in [14]. Consider distinct points $a, b, c, d \in \mathbb{C}$ and define the *cross-ratio* of a, b, c , and d as

$$(2.16) \quad \rho(a, b, c, d) = \frac{(d - a)(b - c)}{(c - d)(a - b)}.$$

This definition extends to $\hat{\mathbb{C}}$. If $d = \infty$, then $\rho(a, b, c, \infty) = -(b - c)/(a - b)$ and we get analogous formulas if any of the other terms are ∞ .

Basic facts about cross-ratios make them of use to the parameter problem. First, the cross-ratio of four points is invariant under a Möbius transformation of $\hat{\mathbb{C}}$. In other words, for Möbius m ,

$$\rho(a, b, c, d) = \rho(m(a), m(b), m(c), m(d)).$$

Second, if a, b, c , and d lie in counterclockwise order on $\partial\mathbb{D}$, then their cross-ratio is necessarily a negative real number. Third, if a, b , and c are on $\partial\mathbb{D}$ in counterclockwise order and x is a negative real number, then there is a unique point $d \in \partial\mathbb{D}$ clockwise from a and counterclockwise from c that satisfies $\rho(a, b, c, d) = x$. The second and third facts are proven in [14] and the first can be shown easily by first proving it for translations, scalings, and inversions and then using the fact that any Möbius transformation is a composition of these three maps.

Using the Cayley transform we get similar results for points on the real line. That is, if a, b, c, d are in order on the extended real line, then their cross-ratio is negative, and if a, b, c are in order on the real line and $x < 0$, then there is a unique $d \in \mathbb{R} \cup \{\infty\}$ to the right of c such that $\rho(a, b, c, d)$.

Suppose we had a triangulation \mathcal{T} of $P \in \mathcal{P}_n$ and the corresponding collection of quadrilaterals \mathcal{Q} . For $j = 1, \dots, n - 3$ normalize three of the prevertices of $Q_j \in \mathcal{Q}$ to $0, 1, \infty$ and have the third, call it a_j , in $(0, 1)$. Then letting

$$(2.17) \quad \rho_j = \rho(0, a_j, 1, \infty) = 1 - \frac{1}{a_j}$$

we get $n - 3$ cross-ratios. These cross-ratios along with \mathcal{Q} are enough to reconstruct the SC parameters. To do so, fix the three of the prevertices of Q_1 to $0, 1, \infty$ in the appropriate way that preserves the orientation. ρ_1 uniquely determines the prevertex of the fourth vertex of Q_1 , which will be $-1/(\rho_1 - 1)$. Now take a Q_j that shares a triangle with Q_1 . They share three vertices and so three of Q_j 's prevertices have already been determined and since we have a corresponding cross-ratio we uniquely determine its fourth. We can continue on in this manner until we have exhausted all of the quadrilaterals in \mathcal{Q} . The n points obtained are the SC parameters for P precisely because the cross-ratios are preserved under Möbius transformations. Therefore, solving for the cross-ratios is equivalent to solving for the parameters.

Now that we have the necessary background material we can move on to a description of the Ahlfors Iteration and to the proof of its convergence.

CHAPTER 3

The Ahlfors Iteration

3.1. Description of the Algorithm

We are now ready to outline the algorithm in detail. In order to increase the accuracy of ϵ -approximations to a target polygonal Riemann surface we will employ the first order approximation of a QC mapping in Lemma 2.2.2. In particular, suppose $P \in \mathcal{P}_n$ with SC mapping $S : \mathbb{H} \rightarrow P$, whose parameters are normalized such that three are $0, 1$, and ∞ . Let $\tilde{P} \in \mathcal{P}_n$ be an approximation to P , with mapping $\tilde{S} : \mathbb{H} \rightarrow \tilde{P}$. Assume $\epsilon > 0$ and $F : \tilde{P} \rightarrow P$ is quasiconformal with $\|\mu_F\|_\infty \leq \epsilon \leq k_1$ from Lemma 2.2.2 and F sends vertices to vertices. Assume $0, 1$ and ∞ are parameters of \tilde{S} and correspond to the $0, 1, \infty$ parameters of S . That is, $F(\tilde{S}(0)) = S(0)$ and similar equalities for 1 and ∞ . Finally, let $f = S^{-1} \circ F \circ \tilde{S}$ and extend f to the lower half plane by reflection. Define the *Ahlfors map*, A_f , by

$$(3.1) \quad A_f(z) = z - \frac{1}{\pi} \int_{\mathbb{C}} \mu_f(w) R(w, z) dA,$$

where $R(w, z) = \frac{z(z-1)}{w(w-1)(w-z)}$. If p_j is a parameter of P and q_j is the corresponding guess from the ϵ -approximation, \tilde{P} , then by Lemma 2.2.2

$$|p_j - A_f(q_j)| \leq C\epsilon^2,$$

where the constant only depends on $|q_j|$.

We will update guess parameters using the Ahlfors map, where the quasiconformal mapping F will be a piecewise affine mapping of triangles. One might ask if we can evaluate μ_f easily, but using the composition formulas in Appendix A.1 shows

$$(3.2) \quad \mu_f(z) = \mu_F(\tilde{S}(z)) \left(\frac{|\tilde{S}'(z)|}{\tilde{S}'(z)} \right)^2.$$

This will be no trouble to calculate since μ_F will be piecewise constant and since we know the guess SC map we can easily evaluate its derivate, which is just a product of complex power functions. Below is a step-by-step description of the algorithm.

The Ahlfors Iteration

- Step 1** Let $P \in \mathcal{P}_n$. Fix a triangulation, \mathcal{T} , of P and the collection of quadrilaterals, \mathcal{Q} , as in Section 2.4. Let \tilde{P}_0 be an ϵ -approximation, $\tilde{\mathcal{T}}_0$ its triangulation compatible with \mathcal{T} , and $\tilde{\mathcal{Q}}_0$ the corresponding quadrilaterals in \tilde{P}_0 .
- Step 2** Fix a SC mapping $\tilde{S} : \mathbb{H} \rightarrow \tilde{P}_k$ and calculate the piecewise affine mapping $L : \tilde{P}_k \rightarrow P$.
- Step 3** Normalize the prevertices of \tilde{P}_k such that three of the prevertices of $\tilde{Q}_j \in \tilde{\mathcal{Q}}_k$ are $0, 1$, and ∞ and the third, a_j , is in $(0, 1)$, such that the three normalized to $0, 1$ and ∞ are either vertices of an overlapping quadrilateral already processed or $j = 1$, in which case, \tilde{Q}_1 is the first quadrilateral to be operated on. Calculate the Schwarz-Christoffel mapping $\tilde{S}_j : \mathbb{H} \rightarrow \tilde{P}_k$. Let $S_j : \mathbb{H} \rightarrow P$ be the corresponding SC map whose parameters are normalized in the same way as \tilde{S}_j 's.
- Step 4** Let $f_j = S_j^{-1} \circ L \circ \tilde{S}_j$. Then f_j is a quasiconformal mapping of \mathbb{H} on itself fixing $0, 1$, and ∞ , and we extend it to all of \mathbb{C} by reflection. Apply the Ahlfors Mapping, A_{f_j} , to a_j and record the cross-ratio

$$\rho_j = \rho(0, A_{f_j}(a_j), 1, \infty).$$

- Step 5** Repeat Steps 3 and 4 for each \tilde{Q}_k until all $n - 3$ quadrilaterals are exhausted.
- Step 6** From the collection $\{\rho_j\}_{j=1}^{n-3}$ construct an $O(\epsilon^2)$ -approximation, \tilde{P}_{k+1} of P , as described in Section 2.4 with the appropriate compatible triangulation and set of quadrilaterals. Repeat Steps 2-6 to the desired accuracy.

Denote one iteration of the algorithm above by \mathcal{A} , so that for $k = 0, 1, 2, \dots$, $\tilde{P}_{k+1} = \mathcal{A}(\tilde{P}_k)$. We shall prove the following theorem.

THEOREM 3.1.1. *Let $P \in \mathcal{P}_n$ with triangulation \mathcal{T} . Then there is a $0 < k_3 < 1$ and a $C_4 < \infty$ such that following holds. If \tilde{P}_0 is an ϵ -approximation of P with $\epsilon \leq k_3$, then the Ahlfors Iteration converges quadratically to the correct Schwarz-Christoffel parameters of P . In other words, for $k = 0, 1, 2, \dots$,*

$$(3.3) \quad d_{QC}(P, \mathcal{A}(\tilde{P}_k)) \leq C_4 d_{QC}(P, \tilde{P}_k)^2.$$

The constants depend on P and \mathcal{T} .

We will prove Theorem 3.1.1 using the Lemmas and Propositions below. First, we need to know that we can create a compatible triangulation of an approximating surface. This will be proven in Proposition 3.2.7. Next, we need Proposition 3.3.3 to bound the dilatation of the QC affine map, L , by a constant times the dilatation of the approximation. This bound will allow us to apply Lemma 2.2.2 to get an estimate on the updated parameter guess in Step 4.

If we started with an ϵ -approximation then each new guess parameter $A_{f_j}(a_j)$ obtained in Step 4 is now $O(\epsilon^2)$ away from the true parameter. But applying Proposition 3.3.3 again allows us to conclude that the updated approximation, $\mathcal{A}(\tilde{P}_k)$, is $O(\epsilon^2)$ from P in the d_{QC} metric, which proves the theorem.

3.2. Controlling Side Lengths

The keys to proving Theorem 3.1.1 are showing that we can take $\epsilon > 0$ small enough such that each of our ϵ -approximations have a compatible triangulation with our target polygon's triangulation and that the affine mapping between polygons is bounded above by a fixed constant times ϵ . In order to prove these key points, we will look at the lengths of the sides of the triangulation and how they change if we perturb the SC parameters by ϵ .

Suppose l is the length of a side of some $T \in \mathcal{T}$ for a fixed SC map $S : \mathbb{D} \rightarrow P$. We may normalize the prevertices of T to the third roots of unity, ξ_k . Then l is equal to $|S(\xi_{k_1}) - S(\xi_{k_2})|$ for some ξ_{k_1} and ξ_{k_2} . Perturbing the vertices of S and renormalizing the parameters corresponding to T back to the ξ_k gives us a new mapping $\tilde{S} : \mathbb{H} \rightarrow \tilde{P}$. Then if

$\tilde{l} = |\tilde{S}(\xi_{k_1}) - \tilde{S}(\xi_{k_2})|$, we have

$$(3.4) \quad \begin{aligned} |l - \tilde{l}| &= \left| |S(\xi_{k_1}) - S(\xi_{k_2})| - |\tilde{S}(\xi_{k_1}) - \tilde{S}(\xi_{k_2})| \right| \\ &\leq \left| S(\xi_{k_1}) - \tilde{S}(\xi_{k_1}) \right| + \left| S(\xi_{k_2}) - \tilde{S}(\xi_{k_2}) \right|. \end{aligned}$$

So, estimating the difference between two SC integrals gives an upper bound on the difference in lengths. This is how we will proceed.

To guarantee that the difference of the two SC integrals in (3.4) above is small, one will need to know that all the corresponding parameters are close and that they are bounded away from the ξ_k . In order to get a lower bound on the distance of the parameters to the ξ_k , we will employ the concept of harmonic measure, ω , which the reader can review in Appendix A.3.

We remark that when we measure length on $\partial\mathbb{D}$ we will use normalized Lebesgue measure so that the length of $\partial\mathbb{D}$ is 1. If E is a measurable set in $\partial\mathbb{D}$, then let $|E|$ denote its length.

LEMMA 3.2.1. *Let I_1, I_2, I_3 be disjoint open arcs in $\partial\mathbb{D}$ with $|I_j| = 1/3$. If $w < \omega(z, I_j, \mathbb{D}) < W$ for each j , then there exists an r depending only on w and W such that $z \in B(0, r)$.*

PROOF. Without loss of generality, we may assume $I_1 = (\exp(4\pi i/3), 1)$, $I_2 = (1, \exp(2\pi i/3))$, and $I_3 = (\exp(2\pi i/3), \exp(4\pi i/3))$. This lemma follows from the fact that if I is an arc on $\partial\mathbb{D}$ then the level set $\{z : \omega(z, I, \mathbb{D}) = c\}$ is the arc of a circle in \mathbb{D} intersecting the endpoints of I in an angle of πc [16]. Figure 3.1 depicts the shaded set $Q_1 = \{z : w < \omega(z, I_1, \mathbb{D}) < W\}$. We know that the possible values of z will lie in $\cap Q_j$. To get an explicit estimate it is easiest to conformally map \mathbb{D} to \mathbb{H} so that 0 is sent to i , 1 to ∞ , $\exp(2\pi i/3)$ to $-\sqrt{3}/3$ and $\exp(4\pi i/3)$ to $\sqrt{3}/3$. The mapping is

$$D(z) = i \frac{1+z}{1-z},$$

the inverse of the Cayley transform.

Under D , the domain $Q_1 \cap Q_2$ is sent to a domain in \mathbb{H} contained in the set bounded by the lines $\tan(\pi w)(x + \sqrt{3}/3)$ and $-\tan(\pi w)(x - \sqrt{3}/3)$, which intersect at $i \tan(\pi w)\sqrt{3}/3$.

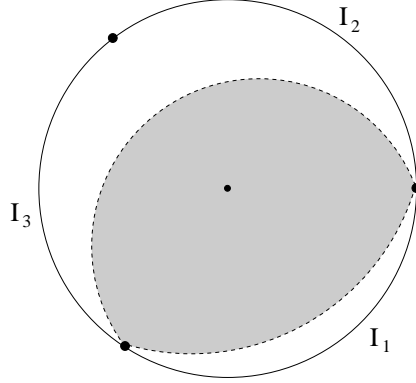


FIGURE 3.1. The set Q_1 in gray.

It remains to bound $D(Q_3)$ away from ∞ . The lower bound on the harmonic measure of I_3 gives us this. The set $\{z \in \mathbb{H} : \omega(z, [-\sqrt{3}/3, \sqrt{3}/3], \mathbb{H}) > w\}$ is the interior of the circle intersecting the endpoints in the angle πw intersected with \mathbb{H} . Our set must be inside this domain and $D(Q_1 \cap Q_2)$. It is easy to check that this intersection is always non-empty. See Figure 3.2.

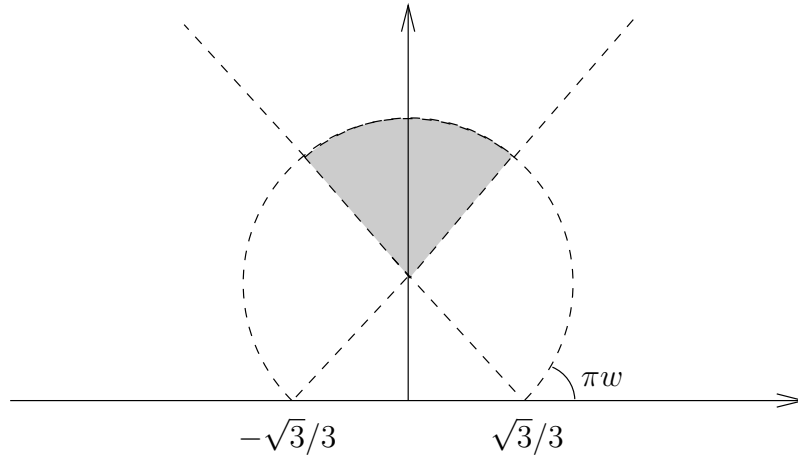


FIGURE 3.2. $D(z)$ must lie in the shaded region if $z \in \cap Q_j$.

So, $D(Q_1 \cap Q_2 \cap Q_3)$ is bounded away from the real axis and away from ∞ . Therefore, there exists an $R' > 1$ such that $D(Q_1 \cap Q_2 \cap Q_3)$ is contained inside of the circle C'_R given by $x^2 + (y - (R'^2 + 1)/2R')^2 = (R'^2 - 1)^2/4R'^2$. These circles all lie in the upper half plane, if $R_1 > R_2$ then C_{R_2} is contained in the interior of C_{R_1} , and $D^{-1}(C_R) = x^2 + y^2 = (\frac{R-1}{R+1})^2$. Therefore, letting $r = (R' - 1)/(R' + 1)$ proves the lemma. \square

For $T \in \mathcal{T}$, denote its centroid by c_T , which we recall is the average of the vertices of T in \mathbb{C} . Let I_T^1, I_T^2 , and I_T^3 be the closure of the open arcs on the boundary of P created when we remove the vertices of T and s_1, s_2 , and s_3 the sides of ∂T such that the endpoints of s_j are the endpoints of I_T^j . A side of the polygonal boundary not in T but containing one of T 's vertices will be called a *neighboring side* of T . See Figure 3.2. If $S : \mathbb{D} \rightarrow P$ is the

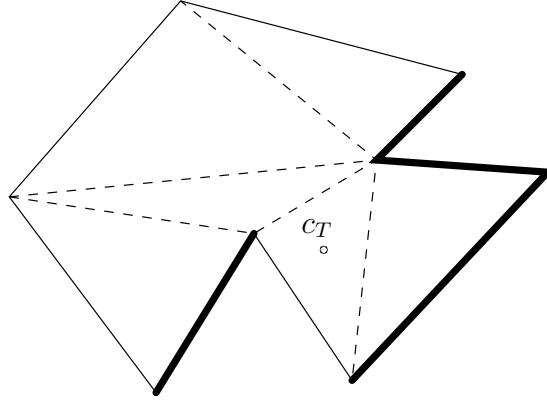


FIGURE 3.3. The neighboring sides of T are highlighted.

SC mapping sending the third roots of unity, ξ_k , to the vertices of T , our next lemma will tell us how close a prevertex can be to the ξ_k . The estimate will depend upon the harmonic measure at c_T of T 's sides and the neighboring sides of T . Thus, for a fixed normalization of the prevertices of T , the other parameters are bounded away by a constant depending only on the local geometry of P near T .

LEMMA 3.2.2. *Let $P \in \mathcal{P}_n$ with triangulation \mathcal{T} . Fix $T \in \mathcal{T}$ and the SC mapping $S : \mathbb{D} \rightarrow P$ sending the third roots of unity, ξ_k , to the vertices of T . Then there exists a $C_5 > 0$ such that any other prevertex of P is at a distance of at least C_5 away from each of the ξ_k . C_5 depends only on the harmonic measure in P at c_T of T 's neighboring sides and the harmonic measure at c_T in T of the sides of T .*

PROOF. First, we want to find upper and lower bounds on $\omega(c_T, I_T^j, P)$ in order to apply Lemma 3.2.1 to get an $r > 0$ such that $S^{-1}(c_T) \in B(0, r)$. For a neighboring side $L \subset I_T^j$, we have $\omega(c_T, I_T^j, P) \geq \omega(c_T, L, P)$. Let w be the smallest $\omega(c_T, L, P)$ over all neighboring sides of T . For our upper bound, if s_j is the side of T corresponding to I_T^j , then note that

$\omega(c_T, I_T^j, P) \leq \omega(c_T, s_j, T)$ by the maximum principle. Letting W be the largest $\omega(c_T, s_j, T)$, we apply Lemma 3.2.1 to find r .

If I is an arc on $\partial\mathbb{D}$ we can use Harnack's inequality, Lemma A.3.1, to compare its length to its harmonic measure at $S^{-1}(c_T)$,

$$\begin{aligned} |E| &= \omega(0, I, \mathbb{D}) \\ &\geq \frac{1 - |S^{-1}(c_T)|}{1 + |S^{-1}(c_T)|} \omega(S^{-1}(c_T), I, \mathbb{D}) \\ &\geq \frac{1-r}{2} \omega(S^{-1}(c_T), I, \mathbb{D}) \\ &= \frac{1-r}{2} \omega(c_T, S(I), P). \end{aligned}$$

A neighboring side L_j not in T is the preimage of an arc I_j in $\partial\mathbb{D}$ with one endpoint ξ_k for some k . The other endpoint is a prevertex q . See Figure 3.2. Let m be the minimum

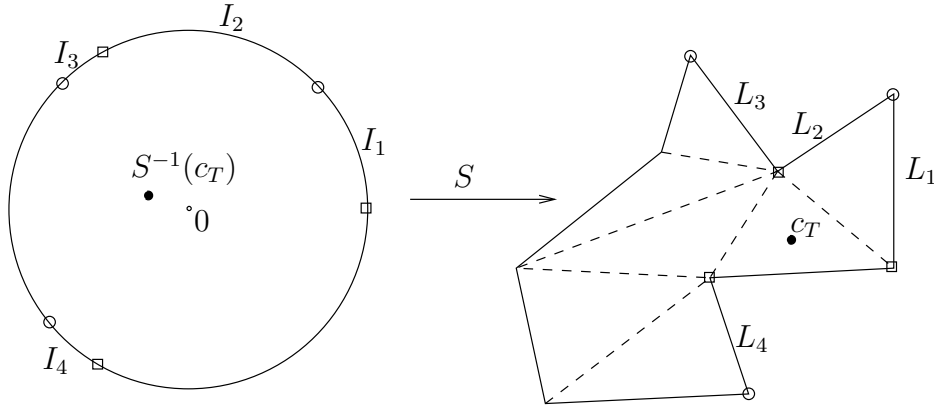


FIGURE 3.4. Bounding the parameter separation. The squares in $\partial\mathbb{D}$ are the third roots of unity.

harmonic measure at c_T of all the neighboring sides of T . Then we have

$$\begin{aligned} |q - \xi_k| &= 2 \sin(\pi |I_j|) \\ &\geq 2 \sin\left(\frac{\pi m(1-r)}{2}\right), \end{aligned}$$

where the first inequality follows from the fact that $2\pi |I|$ is the euclidean length of I and the second follows from the fact that the sine function is increasing from 0 to $\pi/2$. Therefore, the lemma holds with $C_5 = 2 \sin(\pi m(1-r)/2)$. \square

Estimating the difference of two SC integrals will come down to estimating the difference of their integrands, which are just products of complex power functions. We will need the following elementary facts to analyze the difference of the products. The proofs of (3.5) and (3.6) can be found in [20].

LEMMA 3.2.3. *If $0 < x \leq 1$ then*

$$(3.5) \quad 1 + x < e^x < 1 + 2x.$$

Furthermore, if $P_n = \prod_{j=1}^n (1 + a_j)$, where $a_j \in \mathbb{C}$, then

$$(3.6) \quad |P_n - 1| \leq \prod_{j=1}^n (1 + |a_j|) - 1.$$

An estimate on binomial coefficients will also be necessary in the proofs that follow.

LEMMA 3.2.4. *Suppose $\beta \in \mathbb{R}$ and $\beta < 1$. Then there exists a $C_6 = C_6(\beta) > 0$ such that for all $k \in \{1, 2, 3, \dots\}$,*

$$(3.7) \quad \left| \binom{-\beta}{k} \right| \leq \frac{C_6}{k^{1-\beta}}.$$

PROOF. We first take the square of the left hand side in (3.7) and use that fact that the geometric mean is always less than or equal to the arithmetic mean,

$$\begin{aligned} \left| \binom{-\beta}{k} \right|^2 &= \prod_{j=1}^k \left| \frac{-\beta - j + 1}{j} \right|^2 \\ &= \prod_{j=1}^k \left| 1 - \frac{1 - \beta}{j} \right|^2 \\ &\leq \left(\frac{1}{k} \sum_{j=1}^k \left| 1 - \frac{1 - \beta}{j} \right|^2 \right)^k. \end{aligned}$$

Expanding out the terms in the sum gives

$$\begin{aligned}
\left| \binom{-\beta}{k} \right|^2 &\leq \left(\frac{1}{k} \sum_{j=1}^k 1 - 2 \left(\frac{1-\beta}{j} \right) + \left(\frac{1-\beta}{j} \right)^2 \right)^k \\
&= \left(1 + \frac{1}{k} \left(-2(1-\beta) \sum_{j=1}^k \frac{1}{j} + (1-\beta)^2 \sum_{j=1}^k \frac{1}{j^2} \right) \right)^k \\
&\leq \left(1 + \frac{1}{k} (-2(1-\beta) \log k + (1-\beta)^2 \cdot 2) \right)^k.
\end{aligned}$$

The inequalities above follow from the fact that the quantity in the outer parentheses is positive and from the series inequalities

$$\sum_{j=1}^k \frac{1}{j} \geq \log k, \quad \sum_{j=1}^k \frac{1}{j^2} \leq 2,$$

which follow by comparisons with $\int_1^k 1/j dx$ and $\int_1^\infty 1/j^2 dx$, respectively.

It is easy to show by induction that for all positive integers, k if $1 + x/k \geq 0$, then $(1 + x/k)^k \leq e^x$. We then have

$$\begin{aligned}
\left| \binom{-\beta}{k} \right|^2 &\leq \left(1 + \frac{1}{k} (-2(1-\beta) \log k + (1-\beta)^2 \cdot 2) \right)^k \\
&\leq \exp(-2(1-\beta) \log k + 2(1-\beta)^2) \\
&= \left(\frac{e^{(1-\beta)^2}}{k^{(1-\beta)}} \right)^2.
\end{aligned}$$

The lemma then holds with $C_6 = e^{(1-\beta)^2}$. □

Using Lemmas 3.2.3 and 3.2.4 we prove the following lemma that will allow us to estimate the difference between the integrands of Schwarz-Christoffel integrals.

LEMMA 3.2.5. *Fix a positive integer, n , and $\beta_j \in \mathbb{R}$ satisfying $\beta_j < 1$ for $j = 1, \dots, n$. Then there exists a $0 < k_4 = k_4(n, \min_j \beta_j) < 1$ and $C_7 = C_7(n, \min_j \beta_j) > 0$, such that if*

$z_j \in \mathbb{C}$ satisfies $|z_j| \leq \epsilon \leq k_4$ for $j = 1, \dots, n$, then

$$(3.8) \quad \left| \prod_{j=1}^n (1 + z_j)^{-\beta_j} - 1 \right| \leq C_7 \epsilon.$$

PROOF. Let m denote the index of the smallest β_j and set $C = C_6(\beta_m)$ from Lemma 3.2.4. Then let $k_4 = 1/(1 + Cn)$, $C_7 = 4Cn$ and note that $k_4 < 1/2$. Assume that $|z_j| \leq \epsilon \leq k_4$. We use the binomial series expansion and Lemma 3.2.4 to get for all j ,

$$\begin{aligned} \left| (1 + z_j)^{-\beta_j} - 1 \right| &= \left| \sum_{k=1}^{\infty} \binom{-\beta_j}{k} z_j^k \right| \\ &\leq \sum_{k=1}^{\infty} \left| \binom{-\beta_j}{k} \right| |z_j|^k \\ &\leq \sum_{k=1}^{\infty} C \epsilon^k \\ &= C \epsilon / (1 - \epsilon). \end{aligned}$$

Combining (3.6), the inequalities above, and (3.5) we conclude

$$\begin{aligned} \left| \prod_{j=1}^n (1 + z_j)^{-\beta_j} - 1 \right| &\leq \prod_{j=1}^n (1 + |(1 + z_j)^{-\beta_j} - 1|) - 1 \\ &< \prod_{j=1}^n (1 + C \epsilon / (1 - \epsilon)) - 1 \\ &\leq \prod_{j=1}^n \exp(C \epsilon / (1 - \epsilon)) - 1 \\ &= \exp(C n \epsilon / (1 - \epsilon)) - 1 \\ &\leq \frac{2C n \epsilon}{1 - \epsilon} \leq C_7 \epsilon. \quad \square \end{aligned}$$

With the preliminaries complete, we can now show that if we have a polygonal Riemann surface, P , with a triangulation, \mathcal{T} , such that the SC parameters of $S : \mathbb{D} \rightarrow P$ are normalized so the vertices of $T \in \mathcal{T}$ are the images of the third roots of unity and if the other vertices are perturbed by some $\epsilon > 0$ to get a new SC map \tilde{S} , then we can make the distance between the vertices of T and the corresponding images of \tilde{S} close up to $O(\epsilon)$.

PROPOSITION 3.2.6. Let $P \in \mathcal{P}_n$ with triangulation \mathcal{T} and fix $T \in \mathcal{T}$. Let $S : \mathbb{D} \rightarrow P$ be the SC mapping with parameters, $\{p_j\}$, where p_1, p_2 , and p_3 are the third roots of unity, ξ_j , and the prevertices of T . Then there is a $k_5 < 1$ and $C_8 > 0$ such that if $q_j = p_j$, for $j = 1, 2, 3$, and $q_j \in \partial\mathbb{D}$ for $j = 4, \dots, n$ satisfy

$$|q_j - p_j| \leq \epsilon \leq k_5,$$

then the SC mapping \tilde{S} with parameters, $\{q_j\}$, and same angles as S satisfies

$$(3.9) \quad \left| S(\xi_j) - \tilde{S}(\xi_j) \right| \leq C_8 \epsilon,$$

for $j = 1, 2, 3$.

PROOF. By applying a change of variables in the integrals below, we only need to consider the case when $\xi_j = 1$. We'll take k_5 and C_8 to be the smallest and largest, respectively, that works for each of the ξ_j . Let $\alpha_j \pi$ be the interior angles and $\beta_j = 1 - \alpha_j$.

By Lemma 3.2.2 there exists a $C_5 > 0$ such that for each $j \geq 2$, $|p_j - 1| > C_5$. From this, we immediately know there exists a $C_9 \leq 1$ such that for all $x \in [0, 1]$ and $j \geq 2$, $|p_j - x| > C_9$. Let $k_5 = C_9 k_4$, where k_4 is from Lemma 3.2.5 using β_2, \dots, β_n . Let I denote the integral

$$(3.10) \quad I = \int_0^1 (1-x)^{-\beta_1} dx.$$

Note that I is always finite since $\beta_1 < 1$. Finally, assume for $\epsilon > 0$, $|p_j - q_j| \leq \epsilon \leq k_4$. Then

$$\begin{aligned} \left| S(1) - \tilde{S}(1) \right| &= \left| \int_0^1 \left(\prod_{j=1}^n \left(1 - \frac{x}{p_j} \right)^{-\beta_j} - \prod_{j=1}^n \left(1 - \frac{x}{q_j} \right)^{-\beta_j} \right) dx \right| \\ &\leq \int_0^1 (1-x)^{-\beta_1} \prod_{j=2}^n \left| 1 - \frac{x}{p_j} \right|^{-\beta_j} s(x) dx \\ &= \int_0^1 (1-x)^{-\beta_1} \prod_{j=2}^n |p_j - x|^{-\beta_j} s(x) dx, \end{aligned}$$

where

$$s(x) = \left| \prod_{j=2}^n \left(1 + x \frac{1 - p_j/q_j}{p_j - x} \right)^{-\beta_j} - 1 \right|.$$

For all $j = 2, \dots, n$ and $x \in [0, 1]$ we have

$$\left| x \frac{1 - p_j/q_j}{p_j - x} \right| \leq \frac{|q_j - p_j|}{|p_j - x|} \leq \frac{\epsilon}{C_9} \leq k_4.$$

Lemma 3.2.5 gives $s(x) \leq C_7\epsilon$ for all $x \in [0, 1]$.

The term

$$\prod_{j=2}^n |p_j - x|^{-\beta_j}$$

is bounded above by a constant $C < \infty$ because the terms with negative powers are bounded by $C_9^{-\beta_j}$ and the terms with positive powers are bounded by $2^{-\beta_j}$.

Letting $C_8 = ICC_7$ gives

$$\begin{aligned} |S(1) - \tilde{S}(1)| &\leq \int_0^1 (1-x)^{-\beta_1} \prod_{j=2}^n |p_j - x|^{-\beta_j} s(x) dx \\ &\leq \int_0^1 (1-x)^{-\beta_1} C C_7 \epsilon dx \\ &= C_8 \epsilon. \end{aligned} \quad \square$$

We may use the previous lemma to prove the existence of compatible triangulations.

PROPOSITION 3.2.7. *Fix $P \in \mathcal{P}_n$ and a triangulation \mathcal{T} . Then there exists a $k_6 = k_6(P, \mathcal{T})$ such that if \tilde{P} is an ϵ -approximation of P with $\epsilon \leq k_6$, there exists a compatible triangulation of \tilde{P} .*

PROOF. Recall from Lemma 2.3.1 that if for each triangle in \mathcal{T} the corresponding vertices in \tilde{P} have the same orientation, then there is a compatible triangulation.

Fix $S : \mathbb{D} \rightarrow P$ such that $S(\xi_k)$ are the vertices of $T \in \mathcal{T}$, and let a denote T 's least altitude. If the corresponding vertices of \tilde{P} are at most $a/3$ away from those of T , then they'll have the same orientation. See Figure 3.2. We can guarantee this holds using Lemma

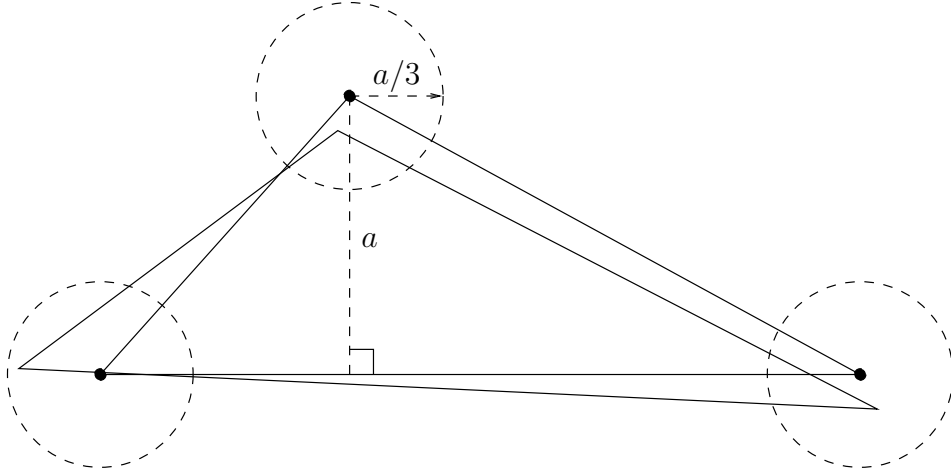


FIGURE 3.5. Preserving the orientation of the triangle.

2.2.3 and Proposition 3.2.6. Indeed, let

$$k = \min(k_2, k_5/C_3, a/(3C_8C_3)).$$

and assume there exists a $(1 + \epsilon)$ -QC mapping, f , of the disk to itself fixing the third roots of unity, which are the prevertices of T , and sends all the SC parameters of P to those of \tilde{P} . If $\epsilon \leq k$ then we know for all $\zeta \in \partial\mathbb{D}$

$$|f(\zeta) - \zeta| \leq C_3\epsilon \leq k_5.$$

By Proposition 3.2.6

$$\left|S(\xi_j) - \tilde{S}(\xi_j)\right| \leq C_8C_3\epsilon \leq a/3,$$

which implies that the vertices of \tilde{P} corresponding to those of T are in the same orientation.

Therefore, let k_6 be the smallest k that works for every $T \in \mathcal{T}$. □

Now that we know we can make the distance between corresponding vertices as close as we want, and hence, the difference between side lengths of triangles, we need to know how this relates to the dilatation of a piecewise affine mapping between surfaces.

3.3. Triangles

When we construct the piecewise mapping of an approximate polygonal Riemann surface to the target surface we need to know estimates on the dilatations. In particular, does a small $\epsilon > 0$ imply that the affine map from an ϵ -approximation has a dilatation bounded by $O(\epsilon)$? The answer to this is yes, and will be confirmed by showing how the lengths of triangles quantitatively relate to the angles, and then how the angles relate to the dilatation of the affine maps.

LEMMA 3.3.1. *Let T and T' be triangles in \mathbb{C} with vertices $\{v_i\}$ and $\{v'_i\}$, respectively, and let l be the minimum of the side lengths of T' . Denote the interior angles by $\{\theta_i\}$ and $\{\theta'_i\}$. There exists a $k_7 = k_7(l) > 0$ and $C_{10} = C_{10}(l) < \infty$ such that if $\epsilon \leq k_7$ and*

$$|v_i - v'_i| \leq \epsilon,$$

then for all i ,

$$(3.11) \quad |\theta_i - \theta'_i| \leq C_{10}\epsilon \leq 1.$$

PROOF. Let $k_7 = l/10$, $C_{10} = 10/l$ and assume that for all i , $|v_i - v'_i| \leq \epsilon \leq k_7$. By translating both triangles so $v_1 = v'_1 = 0$ and rotating both by $-\arg v'_2$, we may assume v'_2 is a positive real number and for $i = 2, 3$, $|v_i - v'_i| < 2\epsilon$. Let $\gamma = \arg v_2$, $\beta = \theta'_1 - \gamma$, and $\alpha = \arg v_3 - \theta'_1$. Then $\theta_1 = \alpha + \beta$ and $\theta_1 - \theta'_1 = \alpha - \gamma$. See Figure 3.6.

We'll derive an estimate for $\sin \gamma$, which also hold for $\sin \alpha$ by symmetry.

$$\begin{aligned} |\sin \gamma| &= \frac{|\operatorname{Im} v_2|}{|v_2|} \leq \frac{2\epsilon}{|v'_2| - 2\epsilon} \\ &\leq \frac{2\epsilon}{l - 2\epsilon} \\ &\leq \frac{5\epsilon}{2l}. \end{aligned}$$

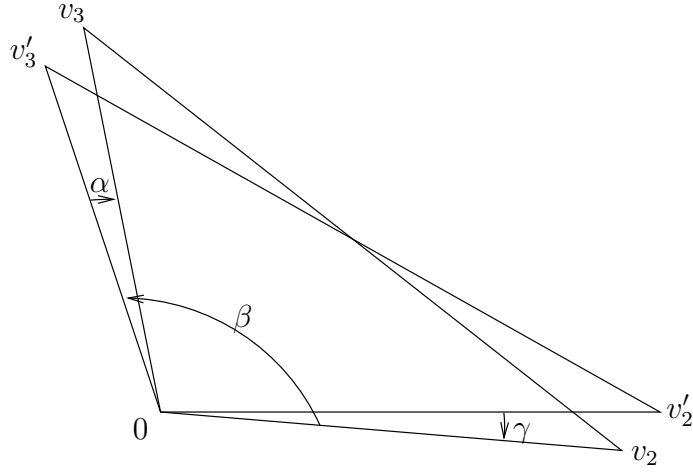


FIGURE 3.6. Triangles and angles in Lemma 3.3.1.

This gives $|\sin \gamma| \leq 1/4$, since $\epsilon \leq l/10$. Furthermore, γ must be acute. If not then $2\epsilon > |v_2 - v'_2| > v'_2 \geq l$, which contradicts our assumption on ϵ . Since γ is acute and $|\sin \gamma| \leq 1/4$, we must have $|\gamma|/2 \leq |\sin \gamma|$, which immediately implies that $|\gamma| \leq 5\epsilon/l$.

Therefore, $|\theta_1 - \theta'_1| = |\alpha - \gamma| \leq C_{10}\epsilon$. We get the same estimates for the other angles depending on which vertex we translate to the origin, which allows us to conclude that (3.11) holds for our choice of k_7 and C_{10} . \square

Our next lemma relates the angles of two triangles to the dilatation of the affine linear mapping between them.

LEMMA 3.3.2. *Let T and T' be triangles in \mathbb{C} with vertices $\{v_i\}$ and $\{v'_i\}$, respectively, in counterclockwise order. Denote the interior angles by $\{\theta_i\}$ and $\{\theta'_i\}$, and let $\theta'_m = \min \theta'_i$. Let $L : T \rightarrow T'$ be the complex affine map sending v_i to v'_i and denote its complex dilatation by μ_L . Then there exists a $0 < k_8 = k_8(\theta'_m) < 1$ and $C_{11} = C_{11}(\theta'_m) < \infty$ such that if*

$$|\theta_i - \theta'_i| \leq \epsilon \leq k_8$$

then

$$(3.12) \quad \|\mu_L\|_\infty \leq C_{11}\epsilon.$$

PROOF. By applying Möbius transformations, we may assume $v_1 = v'_1 = 0$ and $v_2 = v'_2 = 1$. Let $z = v_3$, $\zeta = v'_3$, and $\eta = \sin(\theta'_m/2)$. Assume $z, \zeta \in \mathbb{H}$. Let $k_8 = \eta$ and assume $|\theta_i - \theta'_i| \leq \epsilon \leq k_8$. We will need to estimate the difference of the sine and cosine of our

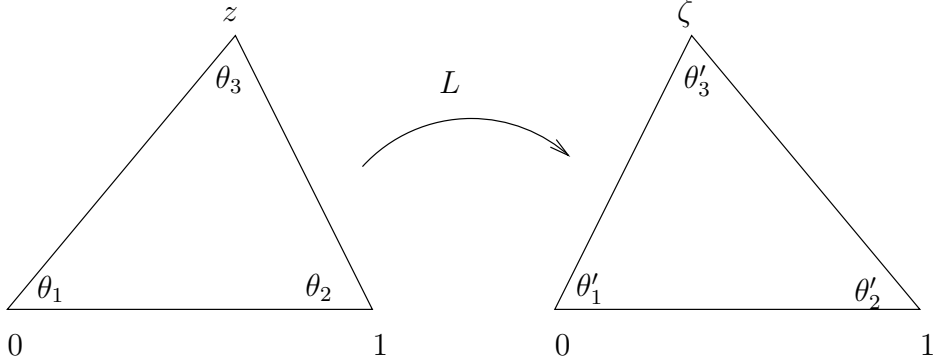


FIGURE 3.7. Triangles T and T' .

angles. Using trigonometric identities and the fact that the difference between our angles is small, we have

$$\begin{aligned} |\sin \theta_i - \sin \theta'_i| &= \left| 2 \sin \left(\frac{\theta_i - \theta'_i}{2} \right) \cos \left(\frac{\theta_i + \theta'_i}{2} \right) \right| \\ &\leq \left| 2 \frac{\theta_i - \theta'_i}{2} \right| = |\theta_i - \theta'_i|, \\ |\cos \theta_i - \cos \theta'_i| &= \left| -2 \sin \left(\frac{\theta_i + \theta'_i}{2} \right) \sin \left(\frac{\theta_i - \theta'_i}{2} \right) \right| \\ &\leq \left| 2 \frac{\theta_i - \theta'_i}{2} \right| = |\theta_i - \theta'_i|. \end{aligned}$$

We have $\theta_i \geq \theta'_i - \epsilon \geq \theta'_m/2$. If $\theta_i \leq \pi/2$, then certainly $\sin \theta_i > \eta$. Suppose we had $\theta_1 > \pi/2$, and $\sin \theta_1 \leq \eta$. If this were true, then we must have $\theta_2 < \pi/2$, $\sin \theta_2 > \eta$ and $|z - 1|$ is the length of the longest side of T . By the law of sines we have $|z - 1| = \frac{\sin \theta_1}{\sin \theta_2} |z|$. $|z - 1| < \frac{\eta}{\eta} |z| = |z|$, which contradicts maximality of $|z - 1|$. So, $\sin \theta_i > \eta$ for every i .

From (2.9) the complex dilatation, μ_L , is given by

$$\mu_L = \frac{z - \zeta}{\zeta - \bar{z}}.$$

Using our estimate for $\sin \theta_1$ and the fact that $z, \zeta \in \mathbb{H}$, we have

$$\begin{aligned}
|\mu_L| &= \left| \frac{z - \zeta}{\zeta - \bar{z}} \right| \leq \frac{|z - \zeta|}{|\operatorname{Im} z|} \\
&\leq \frac{|z - \zeta|}{|z| \sin \theta_1} \\
&\leq \frac{|1 - \zeta/z|}{\eta}.
\end{aligned}$$

We would like to estimate the numerator of the last term above. By the law of sines, $|\zeta| = |\sin \theta'_2 / \sin \theta'_3|$ and $|z| = |\sin \theta_2 / \sin \theta_3|$. So, $|\zeta/z| = |(\sin \theta'_2 / \sin \theta_2)(\sin \theta_3 / \sin \theta'_3)|$. We have

$$\begin{aligned}
\left| \frac{\sin \theta'_2}{\sin \theta_2} \right| &= \left| \frac{\sin \theta'_2 - \sin \theta_2}{\sin \theta_2} + 1 \right| \\
&\leq \frac{|\sin \theta'_2 - \sin \theta_2|}{|\sin \theta_2|} + 1 \\
&\leq \frac{\epsilon}{\eta} + 1.
\end{aligned}$$

Similarly, $\left| \frac{\sin \theta'_2}{\sin \theta_2} \right| \geq 1 - \frac{\epsilon}{\eta}$. The same inequalities hold if we use θ_3 and θ'_3 for θ'_2 and θ_2 , respectively. So,

$$1 - \frac{3\epsilon}{\eta} \leq \left(1 - \frac{\epsilon}{\eta}\right)^2 \leq \left|\frac{\zeta}{z}\right| \leq \left(1 + \frac{\epsilon}{\eta}\right)^2 \leq 1 + \frac{3\epsilon}{\eta}.$$

Using these estimates we have

$$\begin{aligned}
\left| \frac{\zeta}{z} - 1 \right| &= \left| \left| \frac{\zeta}{z} \right| e^{i(\theta'_1 - \theta_1)} - 1 \right| \\
&\leq \left| \left| \frac{\zeta}{z} \right| \cos(\theta'_1 - \theta_1) - 1 \right| + \left| \frac{\zeta}{z} \right| \left| \sin(\theta'_1 - \theta_1) \right| \\
&\leq \left| \cos(\theta'_1 - \theta_1) - 1 \right| + \left| \left| \frac{\zeta}{z} \right| - 1 \right| \cdot \left| \cos(\theta'_1 - \theta_1) \right| \\
&\quad + \left(1 + \frac{3\epsilon}{\eta}\right) \cdot \epsilon \\
&\leq \epsilon + \frac{3\epsilon}{\eta} + \left(1 + \frac{3\epsilon}{\eta}\right) \cdot \epsilon \\
&\leq \left(5 + \frac{3}{\eta}\right) \epsilon.
\end{aligned}$$

Finally,

$$|\mu_L| \leq \frac{1}{\eta} \left| \frac{\zeta}{z} - 1 \right| \leq \left(\frac{5\eta + 3}{\eta^2} \right) \epsilon.$$

Therefore, letting $C_{11} = \left(\frac{5\eta+3}{\eta^2} \right)$ proves the lemma. \square

Combining Proposition 3.2.7 with Proposition 3.2.6 and Lemmas 3.3.1 and 3.3.2 gives the following result.

PROPOSITION 3.3.3. *Let $P \in \mathcal{P}_n$ with a fixed triangulation \mathcal{T} . There exists a $0 < k_9 < 1$ and a $C_{12} < \infty$ such that the following holds. Fix any $T \in \mathcal{T}$ and normalize the prevertices, $\{p_j\}$, of P in $\partial\mathbb{D}$ such that T 's prevertices are the third roots of unity, ξ_j . Suppose that we have an approximation to the SC parameters, $\{q_j\}$, such that the ones corresponding to the vertices of T are also normalized to ξ_j and the rest satisfy*

$$|p_j - q_j| \leq \epsilon \leq k_9.$$

Then letting \tilde{P} denote the approximating surface, there exists a compatible triangulation of \tilde{P} , and the piecewise affine mapping $L : \tilde{P} \rightarrow P$ satisfies

$$(3.13) \quad \|\mu_L\|_\infty \leq C_{12}\epsilon.$$

Proposition 3.3.3 was the last piece for the proof of Theorem 3.1.1. In summary, for a fixed $P \in \mathcal{P}_n$ with triangulation, \mathcal{T} , we can take $\epsilon > 0$ small enough to ensure the existence of a compatible triangulation of an ϵ -approximation and that the affine mapping between the two surfaces is $1 + O(\epsilon)$ -quasiconformal. We then can choose ϵ to be small enough to apply Lemma 2.2.2 and conclude that the updated approximating surface from the Ahlfors Iteration is an $O(\epsilon^2)$ -approximation. Continual application of the iteration gives quadratic convergence.

The last chapter will now detail how to implement the algorithm and present some numerical results.

CHAPTER 4

Implementing the Iteration

4.1. Delaunay Triangulations

Triangulations of polygonal Riemann surfaces are necessary in order to define the piecewise affine mappings in the Ahlfors Iteration. Furthermore, given a $P \in \mathcal{P}_n$, the radius of convergence, $k_3 > 0$, in Theorem 3.1.1 depends on the angles in the initial triangulation of P , in that, larger angles imply a larger radius of convergence. Thus, it is desired to have as large angles as possible in the triangulation.

Suppose Q is a quadrilateral. Then there are only two ways Q can be triangulated by choosing its diagonal. Let's fix a diagonal, so that Q is now decomposed into triangles T_1 and T_2 . Consider the circle C such that the vertices of T_1 are inscribed in it. Let v be the vertex of T_2 not in T_1 . Then either v is contained inside C , v is also inscribed in C , or v is outside of C . We call a diagonal of a quadrilateral *illegal* if the interior of the circle through the vertices of one of the triangles contains the vertex of the other. In such a case, one can *flip* the diagonal to obtain a legal one. See Figure 4.1

We say that a triangulation is *Delaunay* if none of the diagonals are illegal. A Delaunay triangulation always exist and this is easy to show by flipping illegal diagonals (See [11]). Furthermore, if no 4 vertices of P lie on the same circle, then the Delaunay triangulation is unique. If P is a planar n -gon, then there are $O(n \log n)$ algorithms that compute the Delaunay triangulation [8].

A Delaunay triangulation maximizes angles in the following way. Suppose \mathcal{T} is a triangulation of $P \in \mathcal{P}_n$ and denote by $A(\mathcal{T})$ the ordered sequence of $3(n - 2)$ angles, α_j , of the triangles in \mathcal{T} . If \mathcal{T}' is another triangulation, then we say $A(\mathcal{T}') > A(\mathcal{T})$ if there is a j such that $\alpha'_i = \alpha_i$ for $i < j$ and $\alpha'_j > \alpha_j$. If \mathcal{T}_D is a Delaunay triangulation of P and \mathcal{T}

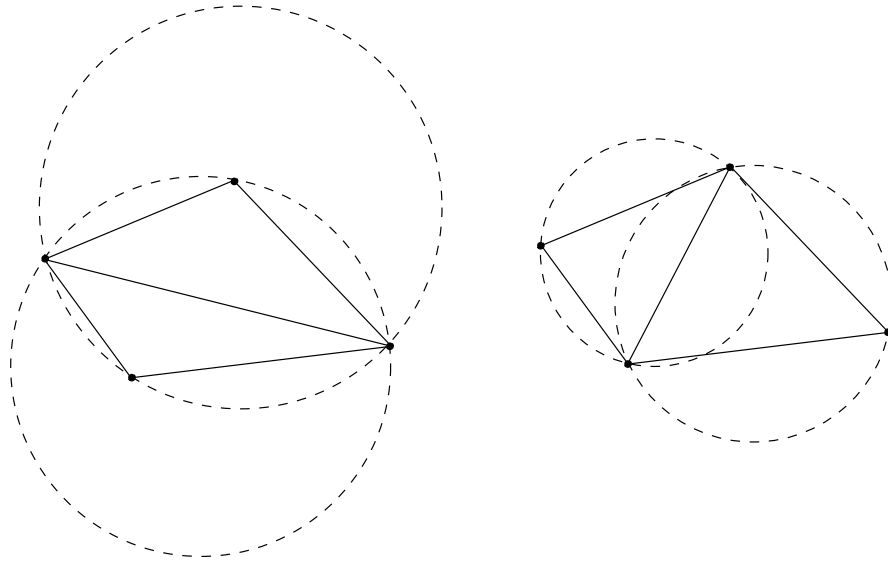


FIGURE 4.1. Flipping the diagonal.

is any other, then $A(\mathcal{T}_D) \geq A(\mathcal{T})$ [11]. So, we see that the Delaunay triangulation in fact maximizes the smallest angle in the triangulation.

4.2. Evaluating SC Mappings

In any implementation of the Ahlfors Iteration it is essential to be able to evaluate Schwarz-Christoffel integrals fast and accurately. A SC integral is a one dimensional line integral and there are *Gaussian quadrature* methods to approximate such integrals. We will mostly follow the treatment of Chapter 3 in [33].

We wish to approximate integrals of the form

$$(4.1) \quad \int_a^b f(x)\omega(x)dx,$$

where f and ω are real-valued functions defined on $(a, b) \subset \mathbb{R}$, f is smooth, and $\omega \geq 0$. ω is called a *weight function*. Consider the following operator

$$(4.2) \quad (f, g) := \int_a^b f(x)g(x)\omega(x)dx.$$

Then (\cdot, \cdot) is an inner product on the vector space, Π_n , of polynomials of degree $\leq n$. So, we may use the Gram-Schmidt process to find $n + 1$ orthonormal polynomials, p_j , of degree j

for $j = 0, \dots, n$ with leading coefficients of 1. Note that p_0 must be the constant 1. Consider the following proposition whose proof can be found in [33].

PROPOSITION 4.2.1. *Let p_0, \dots, p_n be the orthonormal polynomials defined above. Then the following holds.*

- (1) *The n roots, x_1, \dots, x_n , of p_n are real, simple, and lie in (a, b) .*
- (2) *The system of n -equations*

$$\sum_{i=1}^n p_k(x_i)w_i = \begin{cases} (p_0, p_0) & \text{if } k = 0 \\ 0 & \text{if } k = 1, 2, \dots, n-1 \end{cases}$$

has a solution w_1, \dots, w_n such that $w_i > 0$ for all i and for all $p \in \Pi_{2n-1}$,

$$\int_a^b p(x)\omega(x)dx = \sum_{i=1}^n w_i p(x_i).$$

- (3) *If $f \in C^{2n}[a, b]$, then*

$$\int_a^b f(x)\omega(x)dx - \sum_{i=1}^n w_i f(x_i) = \frac{f^{(2n)}(\xi)}{(2n)!}(p_n, p_n)$$

for some $\xi \in (a, b)$.

The roots, x_i , and values, w_i , above are called the *quadrature nodes* and *weights*, respectively.

If we are to evaluate a SC mapping at one of its parameters, the integral may have a singularity. We employ a convenient weighting function as above to handle this case. In particular, let $a = -1, b = 1$, and $\omega(x) = (1-x)^\alpha(1+x)^\beta$, where $\alpha, \beta > -1$. The resulting Gauss quadrature method obtained from the above proposition with this weight is known as *Gauss-Jacobi quadrature*. By applying a change of variables to any of the SC integrals we may use the resulting Gauss-Jacobi quadrature weights and nodes to approximate the SC mapping. As a special case we can also consider the situation when $\alpha = \beta = 0$. We will use this whenever a SC integral needs to be evaluated at some point inside of \mathbb{D} or \mathbb{H} , in which case the integrand has no singularities at the end point.

As we shall see in the next section, the implementation also requires the ability to invert SC mappings. Away from the vertices, where there may be singularities, we can use two methods, either numerically solve an ODE or use Newton's Method.

Suppose we have $S : \mathbb{D} \rightarrow P$. Let $w = S(z)$. Then

$$\frac{dw}{dz} = C \prod_{k=1}^N \left(1 - \frac{z}{p_k}\right)^{-\beta_k}$$

for some nonzero $C \in \mathbb{C}$, where $\beta_k\pi$ is the exterior angle at the k th vertex. But then $z = S^{-1}(w)$ and

$$(4.3) \quad \frac{dz}{dw} = \frac{1}{C} \prod_{k=1}^N \left(1 - \frac{z}{p_k}\right)^{\beta_k}.$$

This is the ODE that will allow us to calculate $S^{-1}(w)$. To do this say we know some $w_0 = S(z_0)$ and the line connecting w_0 and w stays inside of P . Then (4.3) can be solved using standard numerical ODE solvers to obtain $S^{-1}(w)$. See [34].

Since we saw how to evaluate SC integrals with Gaussian quadrature, we can also use Newton's method to evaluate the inverse map. Suppose we want to find $S^{-1}(w)$, or equivalently, we want to find z such that $S(z) = w$. Given some initial guess, z_0 , we can iteratively apply

$$z_{k+1} = z_k - \frac{S(z_k) - w}{S'(z_k)}$$

to solve for the inverse. Newton's method is, of course, not always convergent for an arbitrary initial guess. In order to accurately solve for the inverse, Trefethen [34] advises first applying the ODE to get near the correct solution and then apply Newton's method to increase the accuracy.

Both the ODE and Newton methods for inverting a Schwarz-Christoffel map may behave poorly near vertices because near a vertex, v_k , with interior angle $\alpha_k\pi$, the derivative of the inverse satisfies

$$(S^{-1})'(\zeta) = O\left(\left(\zeta - v_k\right)^{\frac{1}{\alpha_k}-1}\right),$$

which yields a singularity if $\alpha_k > 1$. To avoid this we can derive a representation by utilizing power series.

Say we have a vertex, v , with interior angle, $\alpha\pi$, of a polygonal Riemann surface, P , and let $r > 0$ be small enough so that the sector, $s_{v,r}$, of $B(v, r) \cap P$ of angle $\alpha\pi$ is in the interior of P . Letting w be the immediate vertex counterclockwise from v , define a conformal map, g , from $\mathbb{D} \cap \mathbb{H}$ to $s_{v,r}$ by

$$(4.4) \quad g(z) = \eta r z^\alpha + v,$$

where $\eta = \exp(i \arg(w - v))$. By applying the appropriate Möbius transformations we may assume that P is the image of $S : \mathbb{H} \rightarrow P$ and 0 is the prevertex of v . Then $f = g \circ S^{-1}$ maps the upper half-disk to a neighborhood of 0 intersected with \mathbb{H} . See Figure 4.2

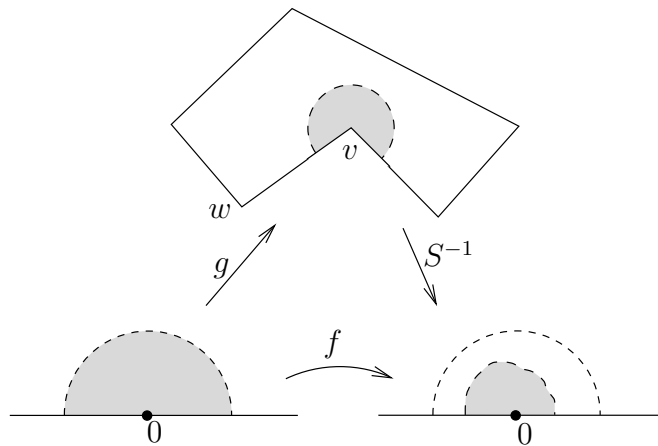


FIGURE 4.2. Defining S^{-1} near corners.

The map f is conformal and extends to the whole disk by the Schwarz reflection principle. Then f has a power series expansion about 0. Write $f = \sum_{j=1}^{\infty} a_j z^j$, then

$$(4.5) \quad S^{-1}(\zeta) = \sum_{j=1}^{\infty} a_j \left(\frac{\zeta - v}{\eta r} \right)^{j/\alpha}.$$

Therefore, it is necessary to know the values for a_j , or at least an approximation to them, and the *discrete Fourier transform* accomplishes this approximation. The following power series discussion comes mostly from [5].

Fix a positive integer N and let R_N denote the N -roots of unity, $w_k = e^{i2\pi k/N}$, for $k = 0, \dots, N-1$. Let $w = w_1$, so that $w_k = w^k$ and $w_k^j = w_j^k$. Let V_N be the vector space of complex-valued functions defined on the N roots of unity. Define $\langle \cdot, \cdot \rangle : V_N \times V_N \rightarrow \mathbb{C}$ by

$$(4.6) \quad \langle f, g \rangle = \frac{1}{N} \sum_{k=0}^{N-1} f(w_k) \overline{g(w_k)}.$$

It is easy to show that (4.6) is an inner product on V_N and that the functions, $e_k(z) = z^k$, for $k = 0, \dots, N-1$, form an orthonormal basis of V_N with respect to this inner product. Therefore, given $f \in V_N$, we may write $f(z) = \sum_{k=0}^{N-1} a_k z^k$, where

$$(4.7) \quad a_k = \frac{1}{N} \sum_{j=0}^{N-1} f(w_j) \overline{w_j^k} = \frac{1}{N} \sum_{j=0}^{N-1} f(w_j) \overline{w_j^k}.$$

The *discrete Fourier transform* (DFT) is defined to be the function sending a sequence of N numbers x_0, \dots, x_{N-1} to another sequence

$$\left\{ \sum_{j=0}^{N-1} x_j \overline{w_k^j} \right\}_{k=1}^{N-1}.$$

This is equivalent to applying the *Fourier matrix*

$$\begin{pmatrix} 1 & 1 & 1 & \dots & 1 \\ 1 & \overline{w_1} & \overline{w_1^2} & \dots & \overline{w_1^{N-1}} \\ 1 & \overline{w_2} & \overline{w_2^2} & \dots & \overline{w_2^{N-1}} \\ \vdots & \vdots & \vdots & \ddots & \vdots \\ 1 & \overline{w_{N-1}} & \overline{w_{N-1}^2} & \dots & \overline{w_{N-1}^{N-1}} \end{pmatrix}$$

to the vector $(x_0, \dots, x_{N-1})^T$. Naive multiplication would take time $O(N^2)$, but there are algorithms called *fast Fourier transforms* (FFT) that only take time $O(N \log N)$ [9]. So, the coefficients (4.7) can be found by taking applying the DFT to $f(w_0), \dots, f(w_{N-1})$ and dividing each result by N .

The goal is to use a power series expansion in order to approximate the inverse of a SC mapping near a vertex. Recall the definition $f = g \circ S^{-1}$, where g is from (4.4), and recall

that f extends to all of \mathbb{D} by a reflection. Assume that f is defined on $B(0, 2)$, which we may do by taking r smaller in the definition of g . Then f is defined on $\partial\mathbb{D}$, so we may use the DFT to obtain a power series $f_0(z) = \sum_{k=1}^{N-1} a_k z^k$. For an arbitrary holomorphic function defined on $D(0, 2)$, this power series does not have to come close to approximating the function. Luckily, because of the conformality of f , it will approximate f .

LEMMA 4.2.2. *Fix a positive integer, N , and suppose g is a conformal map on $D(0, 2)$. Let g_N be the degree $N - 1$ polynomial obtained from g using the discrete Fourier transform. If $r < 1$ and $|z| \leq r$, then*

$$(4.8) \quad |g(z) - g_N(z)| \leq O\left(\frac{1}{N}(\log N + \frac{1}{1-r})\right).$$

PROOF. See [5] page 102. □

Now that we know how to evaluate SC integrals and their inverses we can move on to evaluating the Ahlfors map (3.1).

4.3. Computing the Integral

The difficulty in implementing the Ahlfors Iteration lies with the integral in the Ahlfors map (3.1). Let P denote the target surface with SC map $\Sigma : \mathbb{H} \rightarrow P$, and let $S : \mathbb{H} \rightarrow \tilde{P}$ be a fixed SC map of an ϵ -approximation. The notation for the SC maps has been changed here to ease the calculations that follow. Suppose P and \tilde{P} have compatible triangulations, \mathcal{T} and $\tilde{\mathcal{T}}$, and corresponding piecewise affine mapping, L . Assume that three corresponding parameters of the SC maps are normalized to 0, 1, and ∞ . Then letting $f = \Sigma^{-1} \circ L \circ S$ and

extending it to \mathbb{H}^- , the integral in the Ahlfors map, A_f , is

$$\begin{aligned}
& \int_{\mathbb{C}} \mu_f(z) R(z, w) dA_z \\
&= 2\operatorname{Re} \int_{\mathbb{H}} \mu_f(z) R(z, w) dA_z \\
&= 2\operatorname{Re} \int_{\mathbb{H}} \mu_L(S(z)) \left(\frac{|S'(z)|}{S'(z)} \right)^2 R(z, w) dA_z \\
&= 2\operatorname{Re} \int_{\tilde{P}} \mu_L(\zeta) \left(\frac{|S'(S^{-1}(\zeta))|}{S'(S^{-1}(\zeta))} \right)^2 R(S^{-1}(\zeta), w) J_{S^{-1}}(\zeta) dA_{\zeta},
\end{aligned}$$

where we have made a change of variables, $\zeta = S(z)$, and $J_{S^{-1}}$ is the Jacobian of S^{-1} . For a C^1 homeomorphism, f , of domains in the plane, $J_f = |f_z|^2 - |f_{\bar{z}}|^2$. S^{-1} is conformal, hence, infinitely differentiable and holomorphic, so

$$J_{S^{-1}}(\zeta) = |(S^{-1})'(\zeta)|^2 = 1/|S'(S^{-1}(\zeta))|^2.$$

Using this in the integral above gives

$$\begin{aligned}
& \int_{\mathbb{C}} \mu_f(z) R(z, w) dA_z \\
&= 2\operatorname{Re} \int_{\tilde{P}} \mu_L(\zeta) \left((S^{-1})'(\zeta) \right)^2 R(S^{-1}(\zeta), w) dA_{\zeta} \\
&= 2\operatorname{Re} \sum_{T \in \tilde{T}} \mu_T \int_T \left((S^{-1})'(\zeta) \right)^2 R(S^{-1}(\zeta), w) dA_{\zeta},
\end{aligned}$$

where $\mu_L(z)$ is a constant μ_T on triangle $T \in \tilde{T}$.

The integral has been simplified by changing the domain from \mathbb{C} to the surface, and then using the fact that μ_L is piecewise constant, the integral over the whole polygon has been rewritten as a sum of integrals of holomorphic functions on the triangles in the triangulation.

We can use the holomorphic property of the integrand on triangles to further ease the evaluation of the Ahlfors map. Take a triangle $T \in \tilde{T}$ and consider T as an open set in \mathbb{C} . Decompose T into four pieces as follows. Let s_1, s_2 , and s_3 be disjoint sectors at each vertex of T such that the power series decomposition of S^{-1} is defined at each and let $M = T \setminus \cup s_i$ as in Figure 4.3.

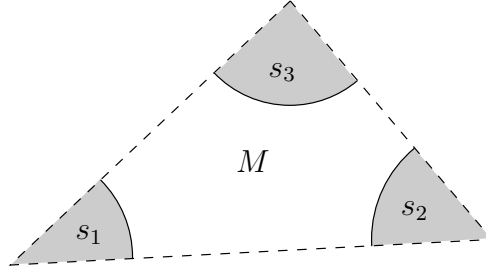


FIGURE 4.3. Decomposing triangles for integration.

Let

$$(4.9) \quad I(\zeta, w) = \left((S^{-1})'(\zeta) \right)^2 R(S^{-1}(\zeta), w).$$

Then, since I is holomorphic in T , we have

$$I(\zeta, w) = \frac{\partial}{\partial \bar{\zeta}} [\bar{\zeta} I(\zeta, w)].$$

This allows the two dimensional integral over M to be reduced to a line integral by appealing to the complex form of Green's formula.

PROPOSITION 4.3.1 (Green's Formula, [2]). *Let Ω be a bounded domain with boundary $\partial\Omega$ consisting of a finite number of disjoint rectifiable Jordan curves. Suppose that f and g are continuous on $\bar{\Omega}$ and have continuous partial derivatives in Ω . Then*

$$(4.10) \quad \int_{\Omega} \left(\frac{\partial f}{\partial z} + \frac{\partial g}{\partial \bar{z}} \right) dA = \frac{i}{2} \int_{\partial\Omega} f d\bar{z} - g dz.$$

So,

$$\begin{aligned} \int_T I(\zeta, w) dA_{\zeta} &= \int_M I(\zeta, w) dA_{\zeta} + \sum_i \int_{s_i} I(\zeta, w) dA_{\zeta} \\ &= -\frac{i}{2} \int_{\partial M} \bar{\zeta} I(\zeta, w) d\zeta + \sum_i \int_{s_i} I(\zeta, w) dA_{\zeta}. \end{aligned}$$

Evaluating the line integral can be done by breaking up the boundary of M into 6 pieces corresponding to the arcs and the line segments and applying regular Gaussian quadrature,

where the weights are the constant 1. Regular Gauss quadrature is used here because $I(\zeta, w)$ is smooth on ∂M .

To calculate the remaining integrals, suppose s is on of the s_i with vertex v and the interior angle of P , not s , is $\alpha\pi$. Assume that the mapping, g^{-1} , in (4.4) sends s to a sector, s' , in \mathbb{D} with radius $1/2$. Recall that in s we can write $S^{-1}(\zeta) = h(g^{-1}(\zeta))$, where h is a conformal mapping of the disk to a neighborhood of $S^{-1}(v)$. So,

$$\begin{aligned} \int_s ((S^{-1})(\zeta))^2 R(S^{-1}(\zeta), w) dA_\zeta &= \\ &= \int_s h'(g^{-1}(\zeta))^2 ((g^{-1})'(\zeta))^2 R(h(g^{-1}(\zeta)), w) dA_\zeta \\ &= \int_{s'} h'(z)^2 R(h(z), w) \frac{|g'(z)|^2}{g'(z)^2} dA_z. \end{aligned}$$

Since

$$R(h(z), w) = \frac{1}{h(z) - w} - \frac{w}{h(z) - w} + \frac{w - 1}{h(z)},$$

we can assume $R(h(z), w) = 1/h(z)$ in the integral and consider the cases when $h(0) = 0$ and $h(0) \neq 0$. Recall $g(z) = \eta r z^\alpha + v$, for real $r > 0$ and $\eta \in \partial\mathbb{D}$. We get

$$(4.11) \quad \int_{s'} \frac{h'(z)^2 |g'(z)|^2}{h(z) g'(z)^2} dA_z = \frac{1}{\eta^2} \int_{s'} \frac{h'(z)^2}{h(z)} \left(\frac{z}{|z|} \right)^{2-2\alpha} dA_z.$$

Now, $h(z)$ can be uniformly approximated using the FFT. This also gives an approximation to $h'(z)$ by simply taking the derivative of the complex polynomial. One can also use the FFT to multiply and divide power series. See Appendix B in [6]. Thus, if $h(0) \neq 0$, we can approximate the integral in (4.11)

$$(4.12) \quad \frac{1}{\eta^2} \int_{s'} \sum_{j=0}^N a_j z^j \left(\frac{z}{|z|} \right)^{2-2\alpha} dA_z,$$

which can be evaluated explicitly over the sector s' by converting the integral to polar form.

If $h(0) = 0$, then $h(z) = \sum_{j=1}^{\infty} b_j z^j$, where $b_1 \neq 0$ since h is conformal. Then $H(z) = z/h(z)$ is holomorphic in \mathbb{D} and can be approximated by a power series by first approximating $h(z)$ using the FFT, factoring out a z , and taking the reciprocal of the resulting polynomial.

Then we can approximate $h'(z)^2 H(z)$ by a power series $\sum_{j=0}^N a_j z^j$ and estimate (4.11) by

$$(4.13) \quad \frac{1}{\eta^2} \int_{s'} \sum_{j=0}^N a_j z^j \frac{1}{z} \left(\frac{z}{|z|} \right)^{2-2\alpha} dA_z,$$

which can also explicitly evaluated by using polar coordinates.

We end this section with a note on the computational complexity of the Ahlfors Iteration for planar n -gons. It is easy to see that, as presented, the Ahlfors Iteration is $O(n^2)$ algorithm. This follows from the fact that for each $n - 3$ cross-ratio we need to calculate $O(n)$ integrals. But do we really have to perform all the $O(n)$ integrals? Because of the crowding of prevertices in polygons with many vertices, some of the line and sector integrals detailed above may add negligible amounts to the total Ahlfors integral and, thus, can be ignored. This is an area where further analysis and study is possible.

4.4. Numerical Results

We now present some numerical results from the implementation of the Ahlfors Iteration. The algorithm was written in Matlab and utilizes Driscoll's *Schwarz-Christoffel Toolbox* [12]. We compare the Ahlfors Iteration with Davis's Method and CRDT. In order to estimate the accuracy of each method, we calculate the affine mapping between the triangulations of the approximate and target polygons, take the largest absolute value of the dilatations (call this value m), and then plot $-\log_{10}(m)$ against the step of each iteration. This roughly tells us how many digits of accuracy each approximations has.

Each method requires an initial guess of the parameters. We use the starting guess of CRDT, which takes the cross-ratios of the quadrilaterals of the triangulated target polygon. As seen earlier, these cross-ratios give us a unique initial guess for the parameters.

Each of the examples below shows the quadratic convergence of the Ahlfors Iteration as guaranteed by Theorem 3.1.1. Furthermore, the Ahlfors Iteration converges in fewer steps than CRDT and Davis's Method. However, the running time of the Ahlfors Iteration is much slower because of the $O(n^2)$ integrals that need to be calculated at each step and because many SC inverses must be found to accurately compute those integrals.

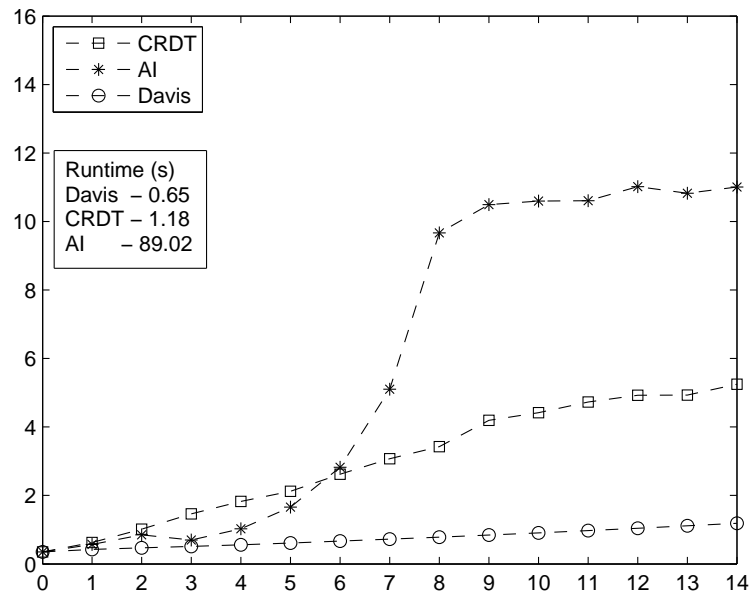
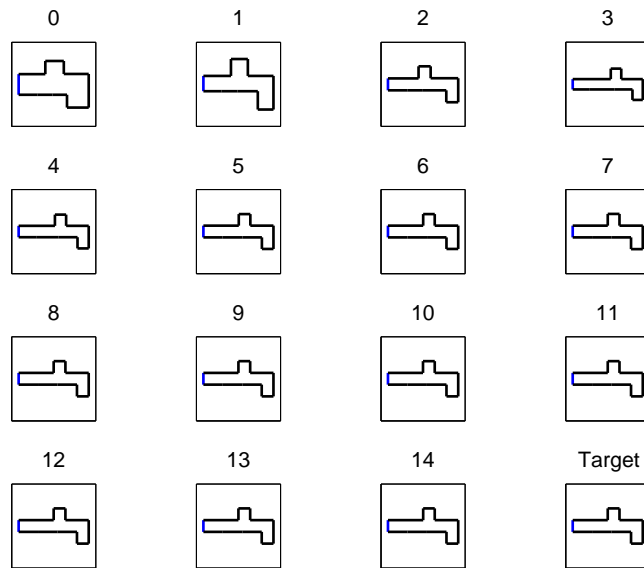


FIGURE 4.4. Above are the approximating polygons for each step of the Ahlfors Iteration and the target polygon. Below is the accuracy of the methods at each iteration.

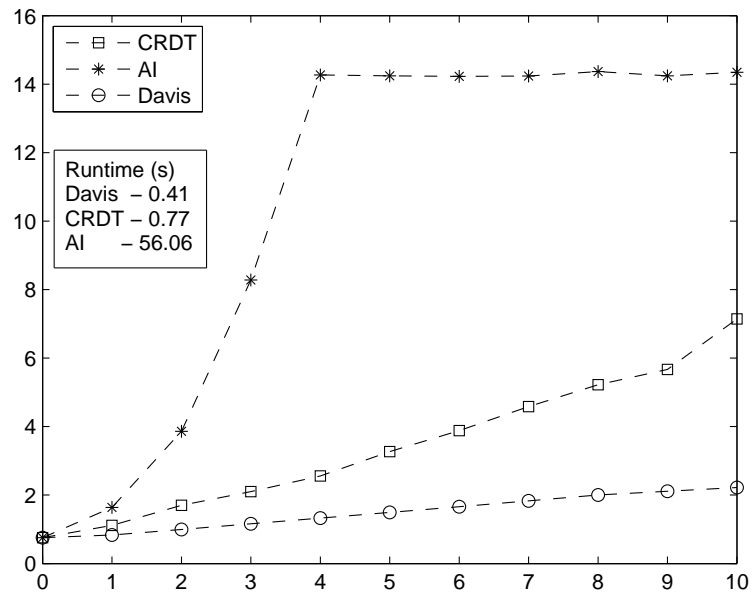
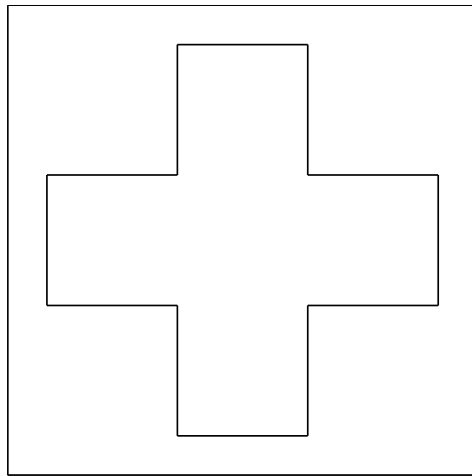


FIGURE 4.5. The quadratic convergence of the Ahlfors Iteration is very pronounced for the polygon above.

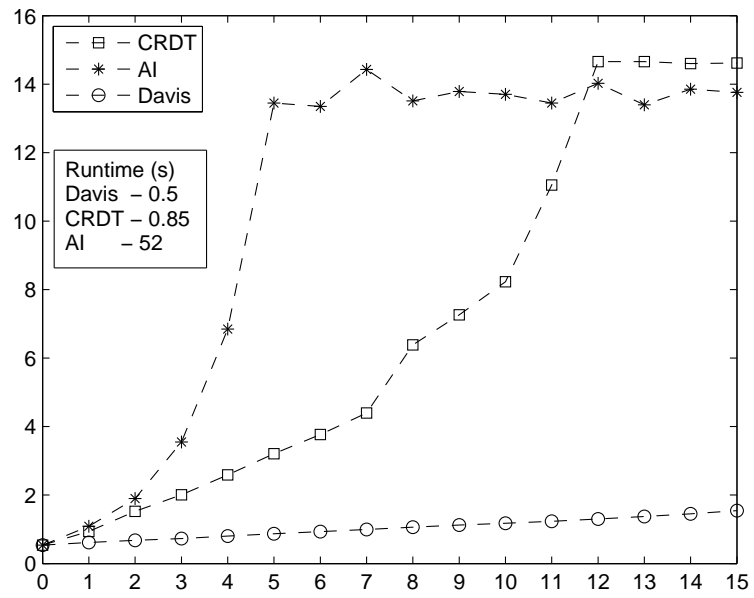
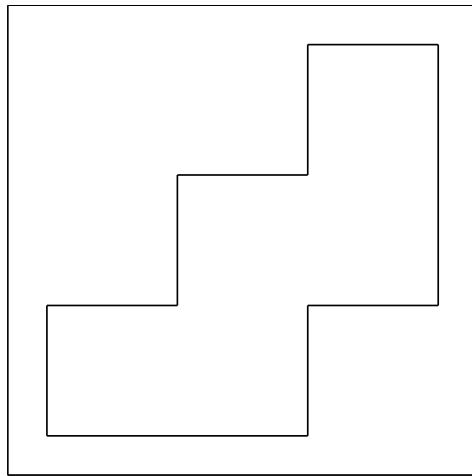


FIGURE 4.6. Again, the Ahlfors Iteration converges in fewer steps.

Bibliography

- [1] Lars V. Ahlfors. *Lectures on quasiconformal mappings*, volume 38 of *University Lecture Series*. American Mathematical Society, Providence, RI, second edition, 2006. With supplemental chapters by C. J. Earle, I. Kra, M. Shishikura and J. H. Hubbard.
- [2] Kari Astala, Tadeusz Iwaniec, and Gaven Martin. *Elliptic partial differential equations and quasiconformal mappings in the plane*, volume 48 of *Princeton Mathematical Series*. Princeton University Press, Princeton, NJ, 2009.
- [3] A. F. Beardon. *A primer on Riemann surfaces*, volume 78 of *London Mathematical Society Lecture Note Series*. Cambridge University Press, Cambridge, 1984.
- [4] Christopher J. Bishop. BiLipschitz approximations of quasiconformal maps. *Ann. Acad. Sci. Fenn. Math.*, 27(1):97–108, 2002.
- [5] Christopher J. Bishop. The riemann mapping theorem. <http://www.math.sunysb.edu/~bishop/classes/math626.F08/rmt.pdf>, 2008. Lecture Notes.
- [6] Christopher J. Bishop. Conformal mapping in linear time. *Discrete Comput. Geom.*, 44(2):330–428, 2010.
- [7] Christopher J. Bishop. Optimal angle bounds for quadrilateral meshes. *Discrete Comput. Geom.*, 44(2):308–329, 2010.
- [8] L. Paul Chew. Constrained Delaunay triangulations. *Algorithmica*, 4(1):97–108, 1989. Computational geometry (Waterloo, ON, 1987).
- [9] James W. Cooley and John W. Tukey. An algorithm for the machine calculation of complex Fourier series. *Math. Comp.*, 19:297–301, 1965.
- [10] R. T. Davis. Numerical methods for coordinate generation based on schwarz-christoffel transformations. *4th AIAA Comput. Fluid Dynamics Conf., Williamsburg, VA*, pages 1–15, 1979.
- [11] Mark de Berg, Otfried Cheong, Marc van Kreveld, and Mark Overmars. *Computational geometry*. Springer-Verlag, Berlin, third edition, 2008. Algorithms and applications.
- [12] Tobin A. Driscoll. Algorithm 843: improvements to the Schwarz-Christoffel toolbox for MATLAB. *ACM Trans. Math. Software*, 31(2):239–251, 2005.

- [13] Tobin A. Driscoll and Lloyd N. Trefethen. *Schwarz-Christoffel mapping*, volume 8 of *Cambridge Monographs on Applied and Computational Mathematics*. Cambridge University Press, Cambridge, 2002.
- [14] Tobin A. Driscoll and Stephen A. Vavasis. Numerical conformal mapping using cross-ratios and Delaunay triangulation. *SIAM J. Sci. Comput.*, 19(6):1783–1803, 1998.
- [15] H. M. Farkas and I. Kra. *Riemann surfaces*, volume 71 of *Graduate Texts in Mathematics*. Springer-Verlag, New York, second edition, 1992.
- [16] John B. Garnett and Donald E. Marshall. *Harmonic measure*, volume 2 of *New Mathematical Monographs*. Cambridge University Press, Cambridge, 2005.
- [17] D. Gilbarg. A generalization of the Schwarz-Christoffel transformation. *Proc. Nat. Acad. Sci. U. S. A.*, 35:609–612, 1949.
- [18] A. W. Goodman. On the Schwarz-Christoffel transformation and p -valent functions. *Trans. Amer. Math. Soc.*, 68:204–223, 1950.
- [19] Jeremy Gray. On the history of the Riemann mapping theorem. *Rend. Circ. Mat. Palermo (2) Suppl.*, (34):47–94, 1994.
- [20] Robert E. Greene and Steven G. Krantz. *Function theory of one complex variable*, volume 40 of *Graduate Studies in Mathematics*. American Mathematical Society, Providence, RI, third edition, 2006.
- [21] Allen Hatcher. *Algebraic topology*. Cambridge University Press, Cambridge, 2002.
- [22] Juha Heinonen. *Lectures on analysis on metric spaces*. Universitext. Springer-Verlag, New York, 2001.
- [23] Juha Heinonen. What is ... a quasiconformal mapping? *Notices Amer. Math. Soc.*, 53(11):1334–1335, 2006.
- [24] L. H. Howell. *Computation of Conformal Maps by Modified Schwarz-Christoffel Transformations*. PhD thesis, MIT, 1990.
- [25] Tadeusz Iwaniec and Gaven Martin. *Geometric function theory and non-linear analysis*. Oxford Mathematical Monographs. The Clarendon Press Oxford University Press, New York, 2001.
- [26] Shizuo Kakutani. Two-dimensional Brownian motion and harmonic functions. *Proc. Imp. Acad. Tokyo*, 20:706–714, 1944.
- [27] O. Lehto and K. I. Virtanen. *Quasiconformal mappings in the plane*. Springer-Verlag, New York, second edition, 1973. Translated from the German by K. W. Lucas, Die Grundlehren der mathematischen Wissenschaften, Band 126.
- [28] Charles B. Morrey, Jr. On the solutions of quasi-linear elliptic partial differential equations. *Trans. Amer. Math. Soc.*, 43(1):126–166, 1938.
- [29] W. F. Osgood. On the existence of the Green's function for the most general simply connected plane region. *Trans. Amer. Math. Soc.*, 1(3):310–314, 1900.

- [30] Roland Schinzinger and Patricio A. A. Laura. *Conformal mapping: methods and applications*. Elsevier Science Publishers B.V., Amsterdam, 1991.
- [31] Eitan Sharon and David Mumford. 2d-shape analysis using conformal mapping. *International Journal of Computer Vision*, 70(1):55–75, 2006.
- [32] Elias M. Stein and Rami Shakarchi. *Complex analysis*. Princeton Lectures in Analysis, II. Princeton University Press, Princeton, NJ, 2003.
- [33] J. Stoer and R. Bulirsch. *Introduction to numerical analysis*, volume 12 of *Texts in Applied Mathematics*. Springer-Verlag, New York, third edition, 2002. Translated from the German by R. Bartels, W. Gautschi and C. Witzgall.
- [34] Lloyd N. Trefethen. Numerical computation of the Schwarz-Christoffel transformation. *SIAM J. Sci. Statist. Comput.*, 1(1):82–102, 1980.
- [35] Jussi Väisälä. *Lectures on n -dimensional quasiconformal mappings*. Lecture Notes in Mathematics, Vol. 229. Springer-Verlag, Berlin, 1971.

Appendix

A.1. Useful Formulas

When using quasiconformal maps, one often encounters the composition of such mappings and needs to know the complex dilatations. Here we compile some useful formulas on the composition of QC mappings found in [1].

Let $\zeta = f(z)$ for a complex-valued f and let g also be complex-valued. Assume both functions are C^1 . Then we have the following chain rules

$$(A.1) \quad \begin{aligned} (g \circ f)_z &= (g_\zeta \circ f)f_z + (g_{\bar{\zeta}} \circ f)\bar{f}_z \\ (g \circ f)_{\bar{z}} &= (g_\zeta \circ f)f_{\bar{z}} + (g_{\bar{\zeta}} \circ f)\bar{f}_{\bar{z}}. \end{aligned}$$

Recall that for a function h , $\mu_h = h_{\bar{z}}/h_z$. From the above equations one derives the following result,

$$(A.2) \quad \mu_{g \circ f} = \frac{f_z}{f_{\bar{z}}} \frac{\mu_{g \circ f} - \mu_f}{1 - \bar{\mu}_f \mu_{g \circ f}}.$$

Therefore, if g is conformal, then

$$(A.3) \quad \mu_{g \circ f} = \mu_f,$$

and if f is conformal,

$$(A.4) \quad \mu_{g \circ f} = \left(\frac{f'}{|f'|} \right)^2 \mu_{g \circ f}.$$

Suppose we have a quasiconformal mapping F and two conformal mappings S and T . Let $f = T \circ F \circ S$. Then using equations (A.3) and (A.4) we see

$$(A.5) \quad \mu_f = (\mu_F \circ S) \left(\frac{|S'|}{S'} \right)^2.$$

The equality (A.5) is essential in computing the Ahlfors Iteration.

A.2. Riemann Surfaces

A *Riemann surface* is a two-real-dimensional connected manifold S with a maximal set of *charts*, $\{U_\alpha, z_\alpha\}_{\alpha \in A}$, such that the *transition functions*

$$f_{\alpha\beta} = z_\alpha \circ z_\beta^{-1} : z_\beta(U_\alpha \cap U_\beta) \rightarrow z_\alpha(U_\alpha \cap U_\beta)$$

are holomorphic whenever $U_\alpha \cap U_\beta \neq \emptyset$. The set $\{U_\alpha\}_{\alpha \in A}$ must be an open cover and each U_α is homeomorphic to an open set in \mathbb{C} .

Let $f : S \rightarrow T$ be a continuous mapping between Riemann surfaces. By definition, f is holomorphic if for every chart $\{U, z\}$ on S and $\{V, \zeta\}$ on T , with $U \cap f^{-1}(V) \neq \emptyset$ the mapping

$$\zeta \circ f \circ z^{-1} : z(U \cap f^{-1}(V)) \rightarrow \zeta(V)$$

is a holomorphic mapping in the classical sense of domains in \mathbb{C} .

A.3. Harmonic Measure

In this section, we compile information about harmonic measure, the tool with which we are able to get estimates in the Ahlfors Iteration based on local geometry of the polygonal Riemann surface.

Let Ω be a simply connected domain in the plane such that $\partial\Omega$ is a Jordan curve. Fix $z \in \Omega$ and let $\varphi : \Omega \rightarrow \mathbb{D}$ be a conformal map guaranteed by the Riemann mapping theorem such that $\varphi(z) = 0$. By Carathéodory's Theorem, [16], φ has a continuous extension to $\partial\Omega$ and φ is a homeomorphism of $\partial\Omega$ onto $\partial\mathbb{D}$. Let $E \subset \partial\Omega$. Then we define the *harmonic measure* of E at $z \in \Omega$ by

$$(A.6) \quad \omega(z, E, \Omega) = \frac{1}{2\pi} |\varphi(E)|,$$

where $|\varphi(E)|$ denotes the Lebesgue measure of $\varphi(E)$ in $\partial\mathbb{D}$. $\omega(z, E, \Omega)$ is well-defined since if ψ is any other conformal map of Ω to \mathbb{D} such that $\psi(z) = 0$, then ψ and φ differ by a rotation which does not change $|\varphi(E)|$.

If we fix $z \in \Omega$, then the function $E \mapsto \omega(z, E, \Omega)$ is a Borel measure on $\partial\Omega$. On the other hand, if we fix $E \subset \Omega$ and allow z to vary, then the function $z \mapsto \omega(z, E, \Omega)$ is harmonic, that is, satisfies

$$\Delta\omega = \left(\frac{\partial^2}{\partial x^2} + \frac{\partial^2}{\partial y^2} \right) \omega = 0,$$

for all $z \in \Omega$. We use this fact when we apply Harnack's inequality in Lemma 3.2.2.

LEMMA A.3.1 (Harnack's Inequality). *Let u be a nonnegative, harmonic function on a neighborhood of $\bar{D}(0, R)$. Then, for any $z \in D(0, R)$,*

$$\frac{R - |z|}{R + |z|} u(0) \leq u(z) \leq \frac{R + |z|}{R - |z|} u(0).$$

PROOF. See Chapter 7 in [20]. □

If $\Omega = \mathbb{D}$ and $z \in \mathbb{D}$, then letting $\varphi(w) = (w - z)/(1 - \bar{z}w)$ we have

$$\begin{aligned} \omega(z, E, \mathbb{D}) &= \frac{1}{2\pi} |\varphi(E)| \\ &= \frac{1}{2\pi} \int_E |\varphi'(e^{i\theta})| d\theta \\ &= \int_E \frac{1 - |z|^2}{|e^{i\theta} - z|^2} \frac{d\theta}{2\pi}. \end{aligned}$$

Applying a change of variables to formula above gives the harmonic measure on $\partial\mathbb{H}$

$$\omega(x + iy, E, \mathbb{H}) = \int_E \frac{y}{(t - x)^2 + y^2} \frac{dt}{\pi}.$$

There is a seemingly unrelated yet equivalent way of defining harmonic measure of a Borel set $E \subset \partial\Omega$. In [26], Kakutani proves that for $z \in \Omega$, $\omega(z, E, \Omega)$ is the same as the probability that a Brownian motion starting at z will hit E before hitting any other boundary component.

For a thorough and captivating treatment of harmonic measure see the book by Garnett and Marshall [16].